ABSTRACT

Title of Document: *In situ* Burning Alternatives

Brian M. Cohen, Master of Science, 2014

Directed By: Dr. Michael J. Gollner, Assistant Professor, Department of Fire Protection Engineering

In situ burns have been used to remove oil spills for decades. They are relatively easy and inexpensive to administer, and are one of the only methods that is effective for crude oil spill remediation over a body of water. There are, however, environmental implications stemming from burning large quantities of crude oil, which has brought about the need for alternative removal techniques.

Skimming and chemical dispersant procedures are frequently employed but have severe limitations and environmental drawbacks. Several new methods have been developed that use elements of nature such as cotton and peat moss, but these are only effective when implemented close to the shoreline. For spills that occur in the middle of the ocean, these processes are rendered useless, and as such, require the implementation of *in situ* burning.

This study assesses a way in which *in situ* burning can be improved in order to minimize the environmental damage that can occur with crude oil removal. Through the research conducted in this thesis, it is proposed that the application of a fire whirl may mitigate the damage while also improving the removal rate of a crude oil spill located on a body of water.

IN SITU BURNING ALTERNATIVES

By

Brian M. Cohen

Thesis submitted to the Faculty of the Graduate School of the
University of Maryland, College Park, in partial fulfillment
of the requirements for the degree of
Master of Science
2014

Advisory Committee:
Professor Michael J. Gollner, Committee Chair
Professor Elaine S. Oran
Professor James A. Milke

Acknowledgements

First and foremost, I would like to thank my parents for their unwavering support throughout this entire process. Their encouragement and selflessness is something for which I am forever indebted. I cannot thank them enough.

I would also like to thank Dr. Michael Gollner, who has guided me every step of the way. From the beginning of the research, to the conclusion of this thesis, he has been a mentor and a friend. It was an absolute privilege to research under Dr. Gollner and I am forever grateful for his leadership.

Additionally, I would like to express my thanks towards Dr. Huahua Xiao, Dr. Elaine Oran, and Dr. Michael Gollner for developing the idea for this thesis. Their guidance and support throughout the entire process was invaluable.

The assistance I received from my fellow graduate students was paramount to the success and completion of my research. I would like to thank Daniel Gorham, Pietro Maisto, Colin Miller, Ajay Sing, and Zhao Zhao for their desire to provide assistance and support with any work in the lab. I would especially like to thank Dan who was always willing to lend a hand during my experiments and provide advice as to how I could improve my data collection.

I would also like to thank Dr. Stoliarov for allowing me to use the microscale load cell and Olga Zeller, our lab technician who was a great help in the lab and was always willing to set aside her experiments in order to assist me with mine.

Finally, to my friends in the Department of Fire Protection Engineering at the University of Maryland, thank you. While I have interacted with dozens of incredible students and faculty members throughout my five years at Maryland, I would like to particularly thank Rob Hanson, Christine Pongratz, and Rosalie Wills, with whom I have spent many an hour studying, laughing, and living, and whose influence has undoubtedly shaped the person I am today.

Table of Contents

List of Figures

List of Tables

Chapter 1: Introduction

1.1 Motivation for Research

Oil spills are extremely hazardous. Often times they impact local wildlife for many years, not to mention the livelihood of thousands who live nearby or depend on the altered environments for their livelihood, such as fisherman. The Deepwater Horizon spill alone killed over 8,000 animals, and is estimated to have done $2.5 billion in damage to the fishing industry in and around the Gulf of Mexico [1]. The 4.9 million barrels of leaked oil was 19 times larger than the infamous Exxon Valdez spill in Alaska in 1989, with oil loss estimated to have been able to heat over 13,000 homes for a year [2]. A total of 411 *in situ* burns were used in an effort to remove the oil, but these burns alleviated barely 20% of the spilled crude oil [2].

The methods employed to remove spilled oil off the surface included *in situ* burning, skimming, and the application of chemical agents. The purpose of this research was to find a more efficient and ultimately more environmentally friendly way to remove oil spilled over open water.

Fuel spills, especially of crude oil, are environmentally impactful. After prolonged water exposure, crude oil can become seemingly impossible to remove as it emulsifies and diffuses into the local environment, potentially jeopardizing marine and bird life. The current removal techniques available to oil response experts are outdated and inefficient, producing copious amounts of soot and other toxic effluents. The goal of the research conducted for this thesis was to improve the burning efficiency of *in situ* burning,

including faster burn times, lower soot and residual production and enhanced fuel collection. To achieve these objectives, an alternative or improvement of the current *in situ* burning method has to be found. Through the research conducted in this thesis, it was discovered that implementing a fire whirl might be a means to improve upon the current *in situ* burning practices as a means to remove oil spills on a body of water. Fire whirls proved not only a more efficient removal technique, but a more environmentally friendly one as well.

1.2 Current Oil Removal Methods

There are several ways in which an oil slick can be removed from a body of water. While many newer methods use plant-based products as absorption tools, *in situ* burning remains a necessary option for removing oil spills when other techniques are not viable or the scale of the fire is so massive as to warrant faster methods of removal.

One of the first methods developed as a way to remove crude oil from a body of water was by way of skimming. Skimming refers to the containment and eventual collection of oil. This is done with the use of buoyant booms that float on the water, limiting the spread of the oil [3]. Once the spill has been controlled, a boat or mechanical rig can be used to scoop or suck the oil from the water and deposit it into vessels.

Another method developed several decades ago involves absorption by way of sorbents. This technique, which was patented in 1972, uses a circular sponge roll that rotates along the surface of the water, absorbing the spilled crude oil [4]. The sponge mechanism can then be squeezed into a container, which extracts the crude oil allowing for additional

removal. There are several issues with this method, however. First, for larger spills, the process of collecting and then extracting hundreds of thousands of gallons of crude oil can take days and even weeks to complete. Secondly, this technique is only effective on calm bodies of water, which can be troublesome in the event that the oil spill is located on an ocean [5].

Another technique that was developed as a way to clean up an oil spill on a body of water is through the use of chemical dispersing agents. These dispersants contain surfactants that help break down the oil into smaller droplets. Once broken down, the natural currents that persist continue to break down the oil into even smaller particulates, which clears it from the surface of the water, helping to ensure that the spilled oil does not reach the shoreline [6]. As is the case with all crude oil removal methods, that is a downside associated with dispersants, which is that heavier crude oils do not disperse nearly as well as lighter oils. Because of this, gasoline or diesel spills – two of the more common petroleum fuels that are spilled – cannot be dispersed easily or effectively, and as such, require alternative removal methods.

It has recently been discovered that cotton – and specifically micronaire cotton – is a great product for removing crude oil spills. Micronaire cotton is an underdeveloped strain that contains more fibers per unit area than basic cotton, which enables more oil to be absorbed [7]. Through experimentation, it has been found that one pound of this type of cotton can absorb 30 pounds of crude oil, which is remarkably efficient. Using cotton on crude oil that spilled on top of a body of water may pose a problem, as the cotton will

also absorb any water that it comes in contact with. This can render the cotton useless, because if it is exposed to the water, it will be unable to absorb any oil. Another concern is what is to be done with the crude oil-soaked cotton once collected. If discarding the oil is the only possible option, then local landfills will be contaminated with potentially hundreds of thousands of pounds of crude oil, which can pose serious environmental and health hazards.

A method that uses natural means as a way to remove oil spills is a process called bioremediation, where naturally occurring microorganisms digest the oil, effectively removing it from the environment. There are issues with using microorganisms, however. The first is that they are only effective when the oil spill is near the shore [8]. The microorganisms cannot break down the oil because the spills are generally too large, but when a spill is broken up, as is usually the case near the shore, the surface area increases, making it easier for the bacteria to digest the crude oil [9]. Another concern is that the microbes could introduce potentially toxic metals into the local ecosystem. Once the oil is digested, the microbes may excrete small quantities of heavy metals that may contaminate the water, marine life, and fishing industry in the area, which could have serious implications on seafood harvesting.

Another natural remediation tool is peat moss. Unlike cotton, peat moss is hydrophobic, so it only absorbs oil. Another advantage of the peat moss is that microbes inside of the plant will begin to break down the oil, which prevents it from leaking out and contaminating the area [10]. Peat moss also allows for easy cleanup. The plant can be

positioned on the surface of the oil where it absorbs the fuel, and then skimmed from the surface, allowing for a quick and environmentally friendly removal process. Unfortunately there is a major drawback with this method, which is that once the moss absorbs the oil, it is rendered useless and is unable to be reused.

A final method for removing a crude oil spill from a body of water is by way of *in situ* burning. *In situ* burning is "in place" burning in that it is used to clean up an oil spill by igniting an area of oil and having the flame spread along the surface of the fuel until all of oil is aflame [11]. There are many advantages to using *in situ* burning as a removal method. First, it is one of, if not the only method that can rapidly remove oil substantial amounts of oil with little manpower. Another distinct advantage is that it prevents the oil from relocating and damaging the shore and coastline, which greatly reduces the potential impact on tourism and seafood harvesting [1]. This helps to ensure the financial stability of both local citizens and communities, which was adversely effected by the Deepwater Horizon disaster. Additional benefits stemming from *in situ* burning include physical damage minimization and almost guaranteed success. With an *in situ* burn, equipment and machinery that would have otherwise been compromised by an oil spill cannot be quickly removed. It also is a more reliable removal technique, so there is less risk that it will not work. For situations in which the fuel spills over open water, the oil needs to be first collected via skimming and then contained in an area to ensure that fuel is thick enough to sustain burning. If the oil layer is not thick enough, then it will not be able to ignite, which would render the removal useless [12]. This can cause problems, as the oil

will begin to emulsify with the water, forming globules that become impossible to ignite and harmful to marine life.

1.3 *In situ* Burning

Extensive research has already been performed regarding the burning of flammable liquids, especially oil-based fuels, over water. The goal of these small-scale in-situ burning tests has primarily been to discern how different fuels burn when parameters such as the crude oil thickness, volume, surface area, etc. are varied. Much of the work completed in these tests helped to institute a baseline for the experiments performed in this thesis.

In a study conducted by Brogaard et. al., several fuels at different depths were put on to the top of a cylindrical container filled with water [13]. The goal of the study was to see how burning efficiency and regression rate are impacted by initial fuel thickness. Through their research, it was found that crude oil thickness plays a pivotal role for both of these factors. Burning efficiency corresponds to the ratio of the amount of fuel remaining after a burn to the initial fuel and can represented as

$$\eta = 100\left(1 - \frac{m_{res}}{m_{ini}}\right), \tag{1}$$

where η represents the burning efficiency, m_{res} the residual mass of fuel and m_{ini} the initial mass of the fuel. It was found that as the fuel thickness increased, so too did the burning rate efficiency. When oil is poured on top of water, an inherent thickness will develop. This is due in large part to the fact that the density of oil is less than water, so it

will float on the surface. A thickness develops because the viscosity of the oil is high enough that it prevents the oil from spreading. The top of the oil layer was ignited in this study by a blowtorch, with oil underneath acting as insulation from the cool water below. The thickness of the oil layer recedes with time after ignition, eventually becoming too thin to the point that heat losses from the oil to the water drops the surface of the oil below the required ignition temperature, subsequently extinguishing the flame [14-15]. Because of this, increasing the fuel depth increased the amount of insulation between the crude oil and the water below, thus increasing the net amount of fuel that is consumed, improving the burning efficiency of the crude oil. An interesting trend was that the efficiency and regression rate trends both plateaued after the crude oil thickness reached 20 mm, which can be conjectured to be the maximum thickness necessary for the crude oil to be completely insulated from the water, afterwards behaving as a thermally-thick fuel layer. This thickness value varies, however, as it is directly related to the surface area of the container in which the crude oil is held and the subsequent size of the fire.

To evaluate the efficiency, remaining unburned fuel was collected using 3M hydrophobic absorption pads. These pads were weighed before and after absorbing residual fuel left after burning and the amount of fuel remaining was divided by the initial fuel, with smaller values indicating increased burning efficiency.

An issue stemming from crude oil spills on bodies of water is weathering and the emulsification of fuel left over water for some time. Weathering refers to the decomposition of the oil, which alters the physical properties, and consequently, the way

in which the fuel burns. Garo et. al. assessed the impact that weathering had on the burning rate properties of crude oil [16]. The researchers weathered oil for four different lengths of time ranging from 0 to 3 days, and then ignited the oil in order to complete a regression rate analysis. To weather the fuel, water was added to the crude oil, which catalyzed the decomposition process.

Their results showed that the rate at which the fuel burns is markedly reduced when the fuel is weathered for longer times. As the crude oil sits in the water, it begins to decompose, slowly forming into small "packets" that are unable to burn. From the data, it is clear that once a spill has been detected, it must be immediately localized and ignited to ensure that as much fuel as possible can be burned.

Another issue with oil weathering and its subsequent decomposition is that it increases the thermal impetus required for ignition [17]. Wu et. al. found a direct correlation between the ignition time of layers of spilled crude oil and weathering, posing a problem for *in situ* burning because as the fuel becomes increasingly weathered it is much more difficult to conduct an *in situ* burn.

First, if the fuel has been emulsifying for days (or weeks), it may be nearly impossible to ignite. Second, assuming the fuel does ignite, the propensity that the flame has to spread would be dramatically reduced, surely limiting the amount of fuel consumed during the *in situ* burn. Third, and most importantly, the weathered crude oil will burn at a reduced rate, which mitigates the usefulness of burning. These potential problems stem from the

fact that once the crude oil begins to weather, it starts mixing with the water, forming globules that become increasingly difficult to burn.

Walavalkar et. al. empirically correlated the weathering time with the burning time for crude oil by testing how the percentage of emulsified water impacts the length of time of the burn [18]. It was found that there is a rapid decline in the burning time with an increase in weathering. For this analysis, the weathering refers to the water content of the emulsified oil. Through their work it was discovered that if the percentage of water increases – which would occur as the crude oil decomposes – the burning time is reduced by a factor of seven. This again illustrates the importance of locating and removing a crude oil spill as soon as possible.

1.3.1 *In situ* Burning Environmental Concerns

There are several issues that stem from employing an *in situ* burn, most of which are environmental, and are due to not only the burning of the fuel, but the residual that is left once the burn is completed. Two of the most pronounced issues are damaging the local plant and wildlife [19]. This has clear long-term implications, as harming the plant life will reduce the available vegetation, ultimately thinning the fish population, especially near the shoreline where many of the plants are located. If this trend is extrapolated, it can be conjectured that a reduction in wildlife could compromise the fishing industry, which could cause a rise in prices. This was evident in the immediate aftermath that stemmed from the Deepwater Horizon spill [1-2, 20].

Another environmental concern that stems from *in situ* burning is the residue that is left over after combustion concludes. This residue can cause serious problems that adversely affect the marine plants and, by extension, wildlife. Crude oil residue has long-term implications in that as it stagnates, it begins to emulsify with the water, which slowly forces it to decompose [18]. This renders any burning useless, as once it mixes with the water, it becomes impossible to ignite. Another issue that occurs with burn residue is that it may sink, potentially harming the organisms that feed and procreate on the bottom of the body of water as the compounds that are left from the residual fuel are toxic [21]. The issue of residual fuel is addressed and evaluated in earnest later in this thesis.

Another serious implication that stems from burning crude oil is the emissions that are generated during burning. It is well known that carbon dioxide is the predominate gas that is produced during complete combustion of hydrocarbon fuels, but additional, potentially carcinogenic gasses may also form. Sulfur- and nitrogen-based compounds including SO_2 and NO_2 are harmful to humans and monitored by quality control administrations including OSHA to ensure human exposure is limited [11]. Along with the human risks that stem from *in situ* burning, are serious environmental risks. Carbon dioxide and monoxide – two of the major products created by crude oil burning – have been linked to ozone depletion, which has been theorized to cause global warming and adverse effects to both humans and agriculture [22]. Another issue with soot is that it can easily be blown downstream, impacting the air quality of the surrounding area, and the health of its citizens. As was the case with residual fuel, soot production was also an aspect that was evaluated extensively and is discussed in detail later in the thesis.

In situ burning has distinct advantages over other crude oil spill-removal methods, but also has inherent disadvantages that accompany any scenario in which something is burned. This thesis assesses ways in which *in situ* burning can be improved through the generation of fire whirls. It was known that a fire whirl will enhance the burning rate for a traditional hydrocarbon pool fire, but it has not been tested for crude oil or on open water. The impact that it would have on residual fuel and soot production is also unknown. The research conducted in this thesis illustrates that fire whirls not only increase the burning rate, but also reduce emissions and residual fuel, indicating that a fire whirl created on a crude oil spill would improve the results *in situ* burning.

1.4 Fire Whirls

Fire whirls have been studied for several decades, and while the mechanisms of formation are somewhat well understood, their formation remains relatively unpredictable and can occur without warning. One of the first documented fire whirls was in 1923, during the Great Kanto Earthquake that took nearly 40,000 lives [23]. This disaster sparked an interest in the study of fire whirls and how and why they are generated.

1.4.1 Fire Whirl Overview

A fire whirl is generated by a circulating air current. In many ways it is similar to a dust devil or a tornado, but with a fire inside whose heat release rate sustains the stable vortex. [24]. In nature, vortices can be generated when a layer of hot air collects in a column and begins to rise. As the column rises, cooler air begins to fill the void left by the hot air, which creates an instability that has the propensity to rotate. Once this rotational motion

commences, a vortex forms, which causes the air column to rotate. This same behavior is exhibited in a fire whirl, with a major difference being that a flame is provides the thermal inertia. It is important to note how a fire whirl begins, as a whirl can start from air and then the fire takes hold or it can develop exclusively from a fire.

Previous fire whirl generation research has been done completely in laboratory settings. The focus of the research ranged from fuel selection and testing configuration to rotational velocity and flame height. The way in which these components were tested and measured is further discussed below.

1.5 Fire Whirl Classification

There have been multiple studies that assess the manner in which a fire whirl can form. Kuwana et. al. evaluated a larger-scale setup where the goal was to test how fuel pan placement impacts the way in which fire whirls develop, as well as to discover the ideal environment necessary to generate a fire whirl [25-26]. The group placed a total of 14 pans, which ranged in size and depth, in a configuration that replicated a Japanese town hit by an earthquake and subsequent fire whirls. The experiments were designed to test how the positioning of certain boundaries impacted the development of a fire whirl. Figure 1.1 is a top view of the setup.

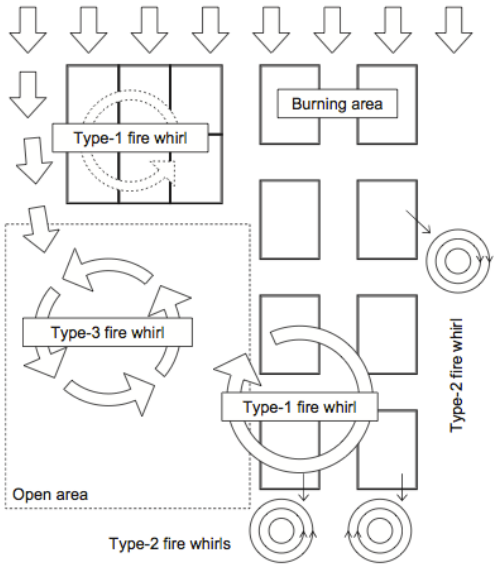

Figure 1.1. Top view of the setup used to classify fire whirls. By Kuwana et. al. [25-26]. Note that the arrows on the top of the figure represent airflow entering the setup by way of a wind tunnel.

Through the analysis, it was found that there are three distinct types of fire whirls that can form, characterized as Type-1, 2, and 3 fire whirls. To produce these whirls, varying sized trays was positioned in the manner illustrated by Figure 1.1. The L-shaped assembly of the containers represented a $1/1000^{th}$ scale model of the fires that enveloped the area after the Great Kanto Earthquake. This specific design allowed for multiple fires, and subsequently, multiple fire whirls to develop. These whirls were classified in three different ways. Type 1 referred to whirls which stabilize for an extended period of time, type 2 a fire whirl formed in an unburned area of the setup but only lasted for a few seconds, and type 3 reflecting a fire whirl that is positioned in an open area and stays active for upwards of five seconds. The most potentially destructive whirl is clearly a type 1 scenario, as the height and intensity of the flame as well as the duration of the whirl are much greater. For the research conducted in this thesis, the fire whirl stabilized

overtop the liquid fuel, which means that the whirl could be classified as Type-1, indicating that the fire whirls generated in our configuration were of high intensity.

Kuwana et. al. also discovered that external airflow had a direct impact on the conditions under which a fire could form. It was found that there was a range of values under which a whirl would develop, and a specific velocity that would generate the strongest possible fire whirl. Through their analysis, they discerned that this critical velocity was dependent on the Froude number, which can be represented as

$$Fr = \frac{m^2}{\rho_o^2 g L} \tag{2}$$

Where m is the mass of fuel consumed per unit burning area per unit time, ρ is the density of ambient air, g is the gravitational constant, and L is the horizontal length scale of the burning area. A correlation was then developed that represented the critical external airflow velocity as a function of the Froude number. The velocity was varied throughout the experiments to find this critical value and it found that, on average, the airflow velocity that would generate fire whirls with the greatest intensity was about 1 m/s. Through their analysis, Kuwana et. al. found that the critical velocity was dependent on a scaled Froude number, which in this case was the Froude number raised to a small power:

$$\frac{U_c}{(gL)^{1/2}} \sim Fr^{n/2}, n \approx .3 \tag{3}$$

It should be noted that the value of *n* ranged between 0.2 and 0.33. External airflow was not used in the research conducted in this thesis, but it is directly related to future work. In order to generate a fire whirl on an open body of water, one proposal is to use four large buoys encircle the crude oil spill. This will allow air to entrain in a circular motion inside of the buoys, which would help generate a fire whirl. The issue is that there may not be enough inherent air entrainment for a whirl to develop, and as such, external airflow would be required to supplement this deficiency with another configuration, such as an L-shaped fire. Because of this, it is critical to know the airflow required to develop the most stable and intense fire whirl to ensure maximum burning efficiency, and the scaling developed in the aforementioned research will assist in this matter.

1.6 Fire Whirl Modeling

It was originally conjectured that fire whirls were generated by atmospheric instabilities and/or the relationship between wind and topography [27]. One of the first studies that actually evaluated how fire whirls develop was completed in 1967 by Emmons and Ying [28]. Their research centered around the impact that angular momentum and airflow circulation had on the development of a fire whirl. They developed an apparatus that would spin a circular mesh, circulating airflow around an acetone fuel source. Through their research it was found that the burning rate increased with an increase in air circulation.

More recently, Zhou et. al. studied several configurations that generated fire whirls merely by positioning additional fires around a central one [29]. The first set of tests

evaluated airflow into a rectangular wall configuration, where the boundaries were made up of ignited fuel pools. Figure 1.2 provides an illustration of the setup that was used.

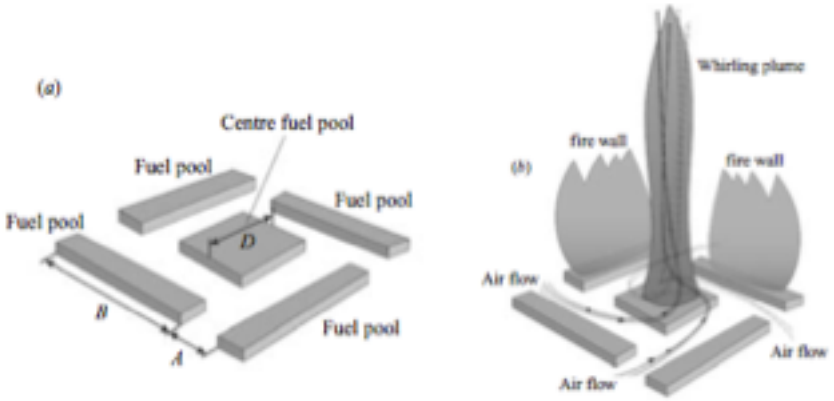

Figure 1.2. Before and after representation of the rectangular fire whirl generation configuration. Reproduced from Zhou et. al. [29].

The four side pool fires produced a flame boundary that resulted in air entrainment in a circular formation at the center. Buoyancy inside of the main plume entrained air from all surrounding plumes. Much of the radial airflow moves across Section A (Figure 1.2), while part travels along and across the flame walls (Section B) (Figure 1.2). This radial flow inward is much stronger than the flow across the fuel pools, which produces a net angular momentum that produces a vortex in the center of the configuration, producing a whirl. The second of the two illustrations in Figure 1.2 demonstrates the impact the airflow has on the generation of a fire whirl.

Additionally, Zhou et. al. tested how these configurations impacted the rotational velocity of the whirl. Configurations ranging from triangular to hexagonal were used in order to distinguish where the highest rotational velocity occurred. The theory that increasing the rotational velocity impacted the flame height stems from previous work completed by multiple research groups [30-32]. It was found that the addition of fire boundaries

increases the rotational velocity of the flame. This was an important finding, for it provided insight into fire whirl generation, mainly that increasing the amount of airflow through openings increases the angular momentum generated by the air, which in turn, increased the strength of the vortex and resulting flame height.

1.6.1 Testing Apparatuses

1.6.1.1 Rotating Mechanism

Much of the research that has been conducted on fire whirls stems from small-scale laboratory apparatuses that function as air entrainment vessels, inducing circulatory airflow and eventually fire whirl behavior. This is practical as it generates repeatable fire whirls at manageable sizes, and also because it is difficult, expensive, and dangerous to generate large fire whirls. With proper scaling analyses, understating the mechanisms of fire whirl generation and behavior is ascertained at the small scale.

In a study completed by Vyalykh et. al., a hand-driven device with an inertia-free coil was developed that allows for consistent spinning of a fire whirl at the base [33]. The apparatus, as shown in Figure 1.4, is a scale model of the experimental setup employed by Emmons and Ying, in that the mechanism housing the fuel rotates, inducing circular airflow and a flame vortex. Utropin, a solid fuel, was tested rather than liquid fuels, so that movement of the liquid fuel was not a factor in the experiments. [34].

Results from testing the design were straightforward in that the height of the flame grew when the apparatus was steadily rotated, and reduced in height when held stationary. From Figure 1.3 it can be seen that introducing an external airflow into the apparatus

slightly increases the flame height. Through their research it was found that inducing the whirl at the base is all that is required for a fire whirl to generate. This was critical as it greatly reduced the time required to develop a repeatable and practical experimental procedure.

Figure 1.3. Snapshots of fire whirl generation. Reproduced from Vyalykh et. al. [33]. Note that the photographs from left to right correspond to the apparatus in stationary position, in a rotating motion, and in a rotating motion with external airflow added, respectively.

1.6.1.2 Line Fire

During the Brazilian wildland fires of 2010, a fire whirl was observed to form and move along a thin flame front. This type of fire whirl had not been seen before. Kuwana et. al. completed a study that assessed how these whirls were developed by attempting to produce them at a small scale experimentally [35]. Through their research it was found that a curved line geometry, such as an L-shape, is necessary for a moving fire whirls to be generated. In their tests, a line of fuel started perpendicular to the flow of air, before aligning with the wind tunnel. This method allowed a fire whirl to not only generate, but move across the fuel path.

The airflow introduced to the system by way of the wind tunnel was of critical importance: too little and a whirl would not form, but too much flow and the flame would topple over, preventing a whirl from forming. Based on the group's analysis, it was found that the velocity of the air that would develop and sustain a fire whirl ranged between 0.15 and 0.35 m/s. This critical threshold was found empirically by conducting the tests, and mathematically by way of scaling. The equation that was used to discover the critical velocity was produced from a collection of formulas that start with a proportionality between velocity and flame height,

$$U_c \sim (gH)^{1/2}, \tag{4}$$

where *H* corresponds to the flame height before the fire whirl occurs. As it cannot be known a priori, it needs to be removed in order to accurately calculate the velocity. The heat release rate per unit area as a function of flame height was then expressed in a correlation as

$$\frac{H}{L} \sim Q^{*2n}, \tag{5}$$

which uses the dimensionless heat-release rate correlation

$$Q^* = \frac{\dot{Q}''}{\rho C_p T (gL)^{1/2}}, \tag{6}$$

where $\dot{Q}^{"}$ is the heat release rate per unit area, ρ, C_p, and T are the density, specific heat, and temperature of the ambient air, respectively, L is the horizontal length scale and n is an empirical constant. Combining equations 4-6 provides a proportionality between the critical velocity and the heat release rate,

$$\frac{U_c}{(gL)^{1/2}} \sim Q^{*n}. \tag{7}$$

Equation 7 therefore provides the critical wind velocity to achieve a fire whirl with a fire of a specific heat release rate in a line-fire configuration.

With the L-shaped fire configuration, Kuwana et. al. were able to generate small-scale fire whirls. Figure 1.4 provides a snapshot of the behavior of the flames both with and without a fire whirl. Note the visible streamlines that develop outside of the line and then inside of it on the "before" picture, and then coalescing into a uniform circular structure in the "after" picture, which helps to form and stabilize a whirl. This experiment was done using a smoke tracer method that was developed by Emori and Saito [36].

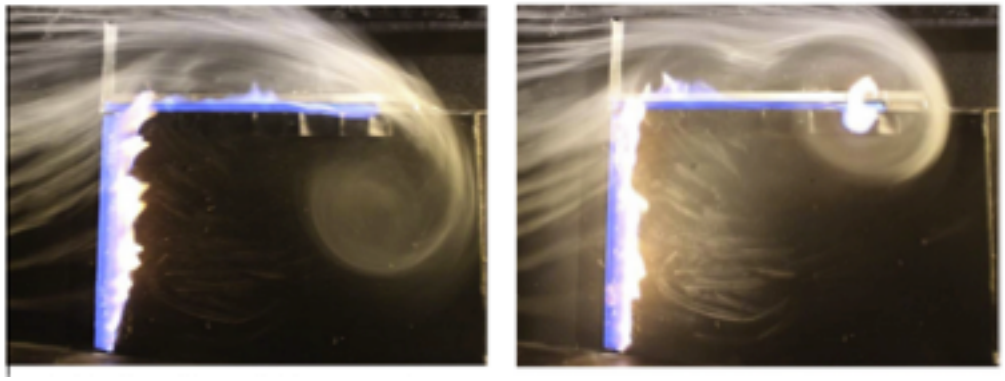

Figure 1.4. Photographs of the streamlines that develop experimentally before and after a fire whirl is generated. Reproduced from Kuwana [35].

Chapter 2: Acetone and Heptane Testing

Instead of experimenting with crude oil immediately, acetone and heptane were used as the initial testing fuels because of their price, availability, and ease of testing compared to crude oil. The purpose of testing with these fuels was to develop a repeatable experimental method that could be employed for crude oil experimentation. A variety of tests ranging from varying the volume of the fuel used in each test to altering the water depth were performed to determine a consistent experimental technique and the efficiency of fire whirls for remediation. In other words, the goal of testing with acetone and heptane prior to crude oil was to discern which testing parameters had the greatest affect on fire whirl generation and burning efficiency.

2.1 Setup

In order to evaluate the effectiveness of fire whirls to increase the burning efficiency of hydrocarbon fuels, the mass loss rate with and without the fire whirl generator were compared. When the ratio of the whirl to non-whirl mass loss rate increased, the parameter that was altered had a positive impact on the fire whirl efficacy, while a reduction in value had a negative impact. The tests were essentially a sensitivity analysis.

To test the mass loss rate, a small cylindrical container was placed on top of a load cell, which was connected to a computer that collected mass data at one-second increments. The fire whirl generation was removed for pool fire experiments.

A sheet of plywood and metal plate were placed in between the container and the load cell, both of which were used as spillage and heat buffers to ensure that the heated fuel-

water mixture and the heat from the flame would not damage the load cell. A metal pan was also used as a small-scale body of water simulator. It had several centimeters of depth, and when filled, was meant to simulate the behavior of water in a pseudo-open body of water environment. This allowed the water to circulate underneath of the fuel, which reflects the scenario where fuel spills on an open body of water. The fuel was contained by a small aluminum ring to ensure a constant surface area of exposed fuel during burning. Figure 2.1 illustrates the fire whirl testing setup. The whirling apparatus was removed when basic pool fire testing was completed. Note that the load cell cannot be seen in this picture but is positioned underneath the setup.

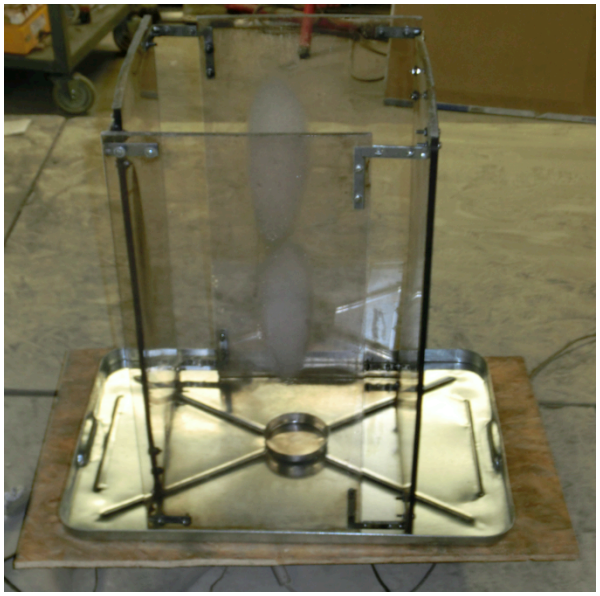

Figure 2.1. Experimental setup for acetone and heptane fire whirl testing.

2.2 Procedure

The first tests that were completed involved placing a specified volume of acetone into a small aluminum dish and then igniting it. Three tests per configuration were completed for 5, 10 and 15 mL volumes of fuel for both fire whirl and non-fire whirl scenarios. This

allowed an average mass loss rate curve to be generated and also demonstrated whether the experimental method was repeatable. It is important to note that acetone was only tested at 10 and 15 mL, as 5 mL of acetone would not achieve a steady burning rate.

For the first set of tests, the aluminum container was filled with water and then covered with a particular volume of fuel. Subsequent tests included hollowing out the bottom of the aluminum container, filling the container and metal pan with water, and then administering fuel overtop the container. This provided a means to test the scenario in which fuel spills onto body of water. Once fuel was added to the container, the mass collection program was initiated and the fuel ignited. After the burning process finished, the program was stopped and the data was exported to an excel file for analysis and post-processing.

As Figure 2.1 illustrates, there are four small slits that enable air to pass through the fire whirl generator. Once the fuel at the center of the fire whirl generator is ignited, air inside the apparatus begins to heat up. This forces the buoyant air and burned gases to rise. As these heated gases move upward, cooler gases are entrained into the apparatus via the four side slits. Because the entraining cooler air still has lateral momentum from entering the slits at a direction parallel with the ground, it enters and subsequently rises in a circulatory manner, forming a vortex, with velocity vectors in both the x- and y- planes. Figure 2.2 provides a simple illustration of this phenomenon. Note that in this figure the fire whirl vessel is circular, but the same principles still apply [37].

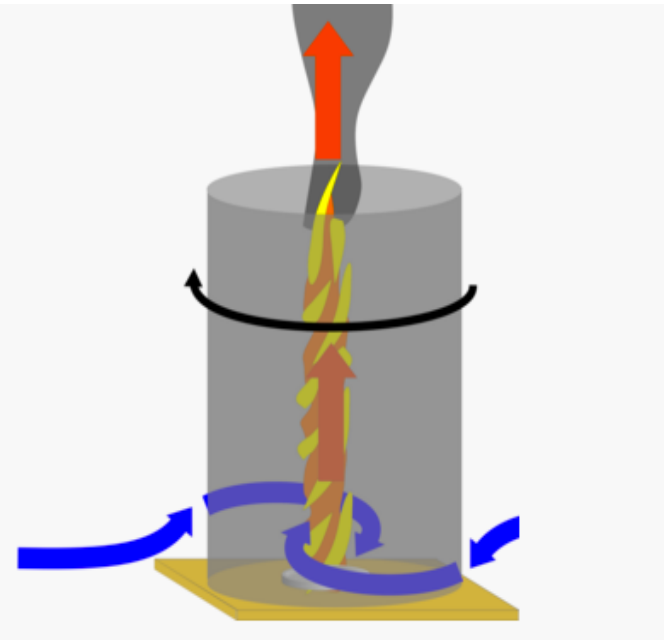

Figure 2.2. Illustration of fire whirl phenomenon with a generated fire whirl [33].

2.3 Results without Water Circulation for Acetone

The first sets of tests were run without water circulation through the bottom of the container. To do this, a small circular aluminum container was filled with a specific amount of acetone and then ignited. The photograph provided in Figure 2.3 demonstrates the simple setup prior to ignition. Three trials were run for each volume of fuel and mass loss rate data were collected and then averaged. These results were then compared to the mass loss rate data from the fire whirl experiments. The setup used for fire whirl testing is provided in Figure 2.1.

Figure 2.3. Experimental setup for acetone and heptane testing without a fire whirl (pool fire configuration).

Figures 2.4 shows the mass loss versus time comparing whirl and non-whirl scenarios for 10 mL of acetone. This figure and all subsequent mass loss plots display mass loss data from at least 3 tests in each configuration averaged every second. A line superimposed on top of the data represents a linear fit of the averaged data taken approximately during the middle 80% of the experiment where burning rates were relatively steady. Mass loss rates, shown in Figure 2.5 were found by determining the slope of the linear fits to the mass loss rate data, with error bars representing the standard deviation between slopes measured from multiple experiments at the same conditions.

As can be seen in the Figures 2.4 and 2.5, and all subsequent mass loss rate plots, the implementation of a fire whirl increases the burning rate of the fuel. This is suspected to occur for several reasons. First, the increased rate of air entrainment near the fuel surface pushes flames closer to the condensed fuel surface, increasing heat feedback, which

increases the rate of vaporization. The flame also forms a favorable view factor with the fuel surface, increasing the radiant heat flux contribution. The air is introduced into the pool fire in a circular motion and is drawn upward due to density and temperature differences while forming into a vortex due to the manner in which the air is entrained.

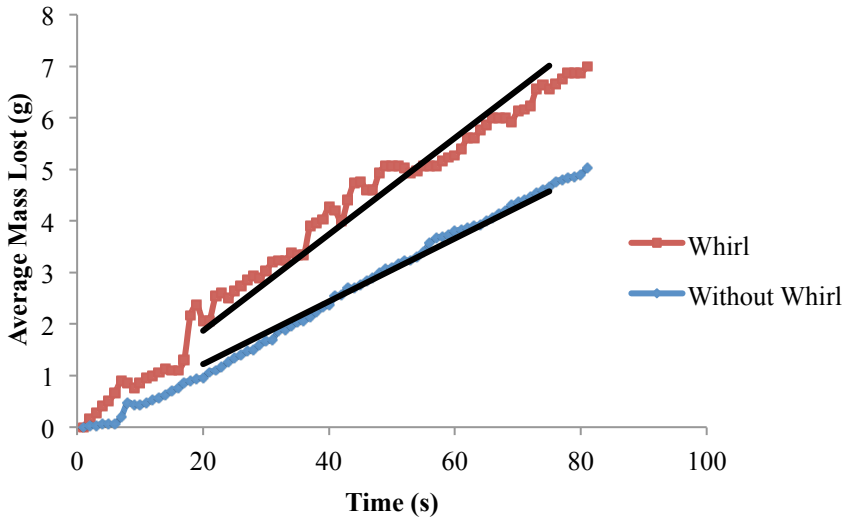

Figure 2.4. Average mass lost for 10 mL of acetone. Lines shown represent linear fits to the middle 80% of the averaged data.

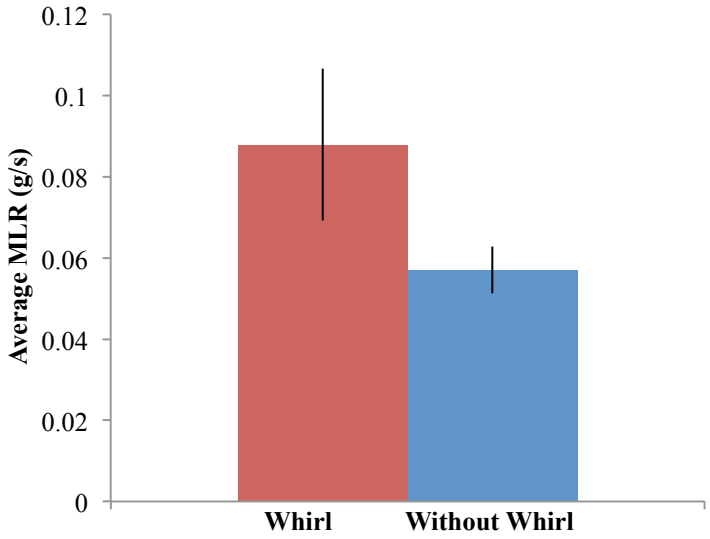

Figure 2.5. Average mass loss rate for 10 mL of acetone.

The values in Figure 2.5 correspond to the slope of the two graphs in Figure 2.4, the average mass loss rate of the fuel during the burn. With a fire whirl, the acetone burned about 35% faster than without it. This sounds like a substantial difference, but as the subsequent figures will illustrate, this change pales in comparison to the effects observed using either heptane or crude oil.

Each experiment was repeated several times, and the average of these tests used in subsequent analysis. The figure also includes the standard deviation of the mass loss rates, which was determined from the repeated mass loss rate experiments. It is interesting to note that the standard deviation for the fire whirl scenario is nearly three times as large as that of the pool fire (non-whirl) simulations. While the deviation is quite small – only about 0.006 g/s – it's still much larger than the pool fire scenario because a fire whirl often has the tendency to generate inconsistent burning. As was mentioned previously, this can occur due to small airflow changes drastically affecting convective

heat transfer and the fuel surface, as well as general stability issues. Velocity shear along the gas/liquid interface induces some circulation in both the fuel and water. Buoyant effects also cause circulation as cooler fuel and water move upward, similar to the behavior observed in pool fires. As the liquid circulates, the cooler water on the bottom reaches the top of the fuel/water mixture, cooling the liquid fuel, which can slow the burning process. This is especially true for crude oil as it has a flash point much higher than the ambient temperature, meaning that additional energy from the fire has to be spent heating the fuel before it can ignite. This effect is amplified with the whirl because the circulatory motion induces greater cooling near the liquid/gas interface. The combination of these factors results in slightly inconsistent burning rates throughout the experiments, especially for fuels with lower burning rates. It is important to note that whirls do not always fully develop into a well-defined vortex, as there is not always enough buoyancy to sustain them. Instead of developing into a distinct whirl, the flame oscillates around the lip of the container.

Figures 2.6 and 2.7 again show average mass lost and mass loss rates for whirl and non-whirl trials, respectively. Here, the amount of acetone is increased to 15 mL.

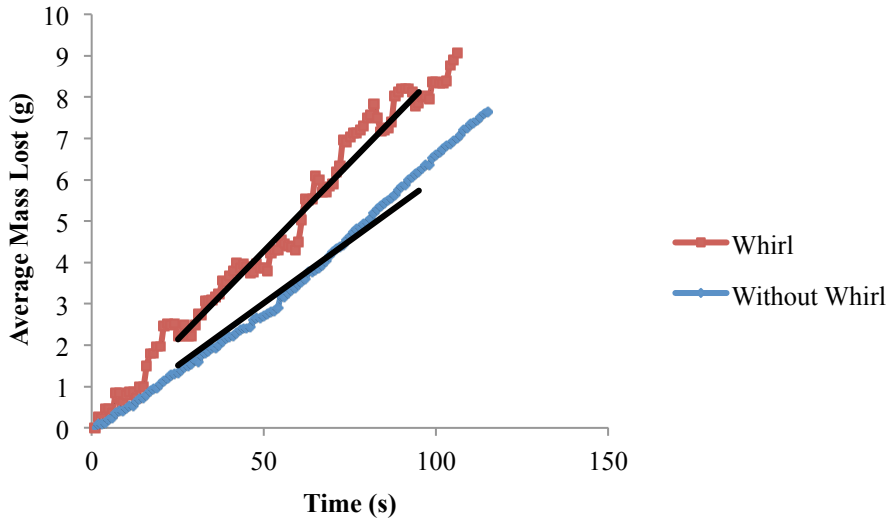

Figure 2.6. Average mass lost for 15 mL of acetone. Lines shown represent linear fits to the middle 80% of the averaged data.

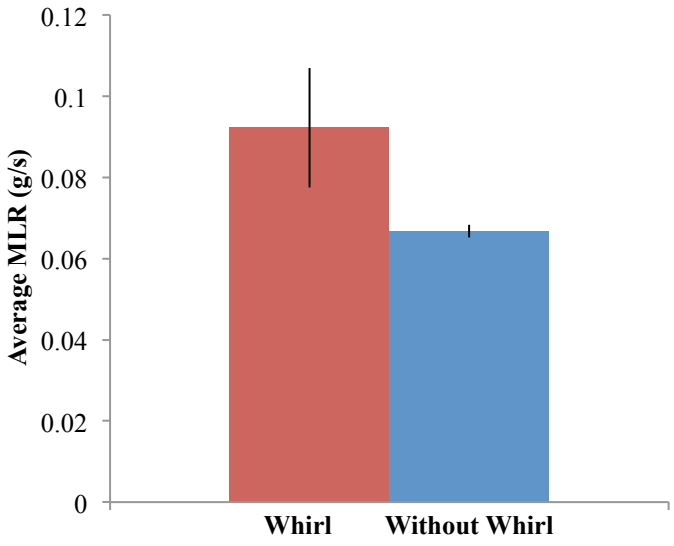

Figure 2.7. Average mass loss rate for 15 mL of acetone.

The ratio between the whirl and non-whirl simulations is actually lower for the 15-mL filled experiments, with an average value of about 17%. It was postulated that this ratio

would actually increase with the addition of more fuel, which is the case for both heptane and crude oil, but for acetone, this was not the case. The mass loss rate for the 15-mL trials increases individually, however, and this can be attributed to several factors. First, with more acetone poured onto the water surface both the volume and surface area of fuel are increased. Increasing the volume of the fuel increases the area the fuel occupies, which increases the area heated and the amount of fuel vapor, leading to a greater burning rate. With a larger fire, the rate of oxygen introduced into the vortex increases, amplifying the effects. With large crude oil tests, the fuel always covered the entire are of the pan, so surface area effects were only important for these preliminary experiments.

Figure 2.8 provides a snapshot of the flame generated by 15 mL of acetone with the addition of the fire whirl apparatus. From the figure it can be seen that the flame generated is more of a pseudo-whirl, in that a clear and distinct whirl is not developed, but rather an elongated flame.

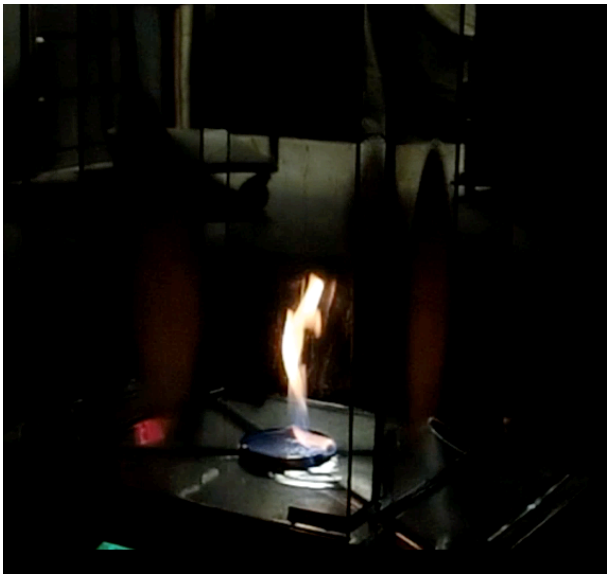

Figure 2.8. Fire whirl generated by 15 mL of acetone.

Figure 2.9 is the combination of Figures 2.5 and 2.7, which compares the average mass loss rates with and without the application of a fire whirl. There is a subtle increase in the mass loss rate as the volume of fuel increases, and the addition of a whirl has an effect as well, but the differences between a whirl and a pool fire without a whirl are not nearly as prominent as in later cases with heptane.

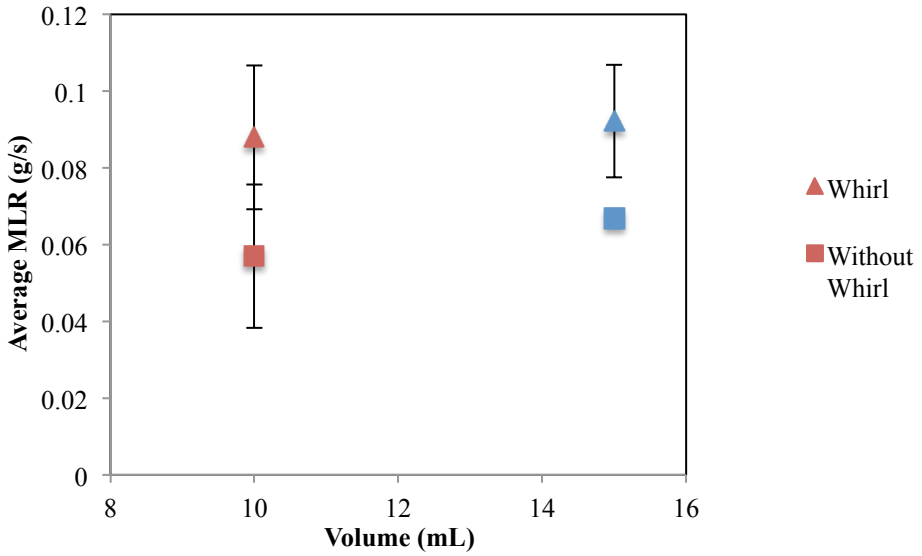

Figure 2.9. Average mass loss rates for 10 and 15 mL of acetone using whirl and non-whirl configurations.

2.4 Results without Water Circulation for Heptane

The same setup that is provided in Figure 2.3 was used for heptane mass loss rate data collection. Figure 2.10 is an illustration of the average mass lost as a function of time for 5 mL of heptane. The differences between the initial and final mass throughout the burn, and the ensuing mass loss rate, are substantially pronounced. As can be seen from Figure 2.10 with 5 mL of heptane, the mass loss rate is nearly twice as large with the addition of a fire whirl. The reason for this difference is due to both the thermal properties of the

fuel, and the resulting fluid mechanics. Acetone has a much lower heat of combustion than the other hydrocarbon fuels that were tested and is also much less sooty, resulting in lowering radiative heat feedback to the other fuel surface, with the net effect of a reduced heat-release rate in comparison to other hydrocarbon fuels. The lower heat-release rate fire therefore has less upward buoyant force and entrains less oxygen from the four slits on the side of the whirl apparatus, which apparently causes insufficient vortex circulation in the center, preventing a discrete fire whirl from forming. Instead, the flame circulates around the outside of the container. This is why acetone was tested at a minimum of 10 mL of fuel – anything less and even a circulating flame would not have formed. Heptane, on the other hand, forms into a well defined fire whirl due to a much higher heat of combustion and radiation heat feedback to the fuel, even without a fire whirl, which is why the difference in mass loss rate is much more pronounced with the addition of a fire whirl. This flame length is then concentrated in the center vortex, and the radiation from the flame is amplified by the addition of a fire whirl – especially due to the view factor with a large flame shape – has a substantial effect on the mass-burning rate. Figure 2.11 is a snapshot of a fire whirl that is developed from 15 mL of heptane. As can be seen from the picture, the flame is much more substantial in size, and a definitive whirling shape can be seen, which was not the case for the acetone flame.

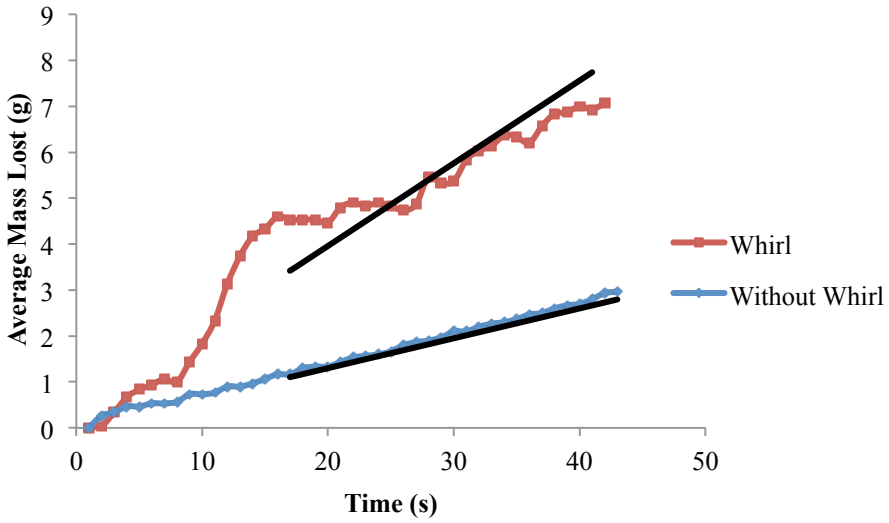

Figure 2.10. Average mass lost as a function of time for 5 mL of heptane. Lines shown represent linear fits to the middle 80% of the averaged data.

Figure 2.11. Fire whirl generated by 15 mL of heptane.

It is important to note the distinction between the whirl and no-whirl experiments. The mass registered by the load cell for the trial in which a fire whirl is generated is much larger than in the case of an experiment where the fire whirl generation apparatus is not used. To ensure that the two mass vs. time plots could be compared, the weight of the fire whirl generation apparatus was subtracted from the total mass. This enabled two distinguishable plots to be compared to one another as a function of time. Figure 2.12 is a comparison of the mass loss rate defined by the slope of the two plots in Figure 2.10.

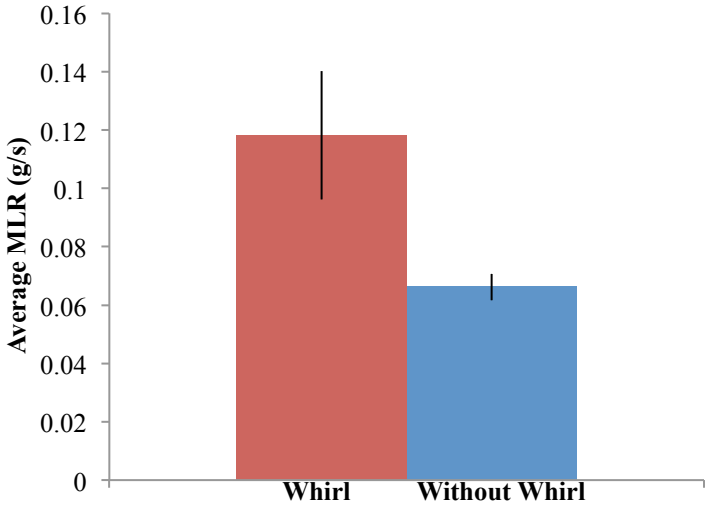

Figure 2.12. Average mass loss rate for 5 mL of heptane.

Figures 2.13 and 2.14 correspond to the mass and average mass loss rate behavior for 10 mL of heptane. Similar to the 5-mL trials, the mass loss rate is much more pronounced with the addition of a fire whirl.

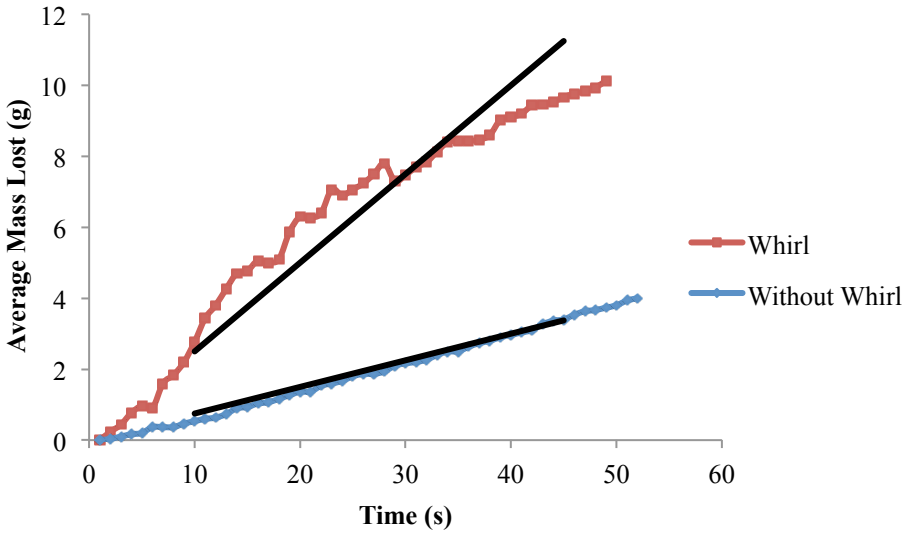

Figure 2.13. Average mass lost as a function of time for 10 mL of heptane. Lines shown represent linear fits to the middle 80% of the averaged data.

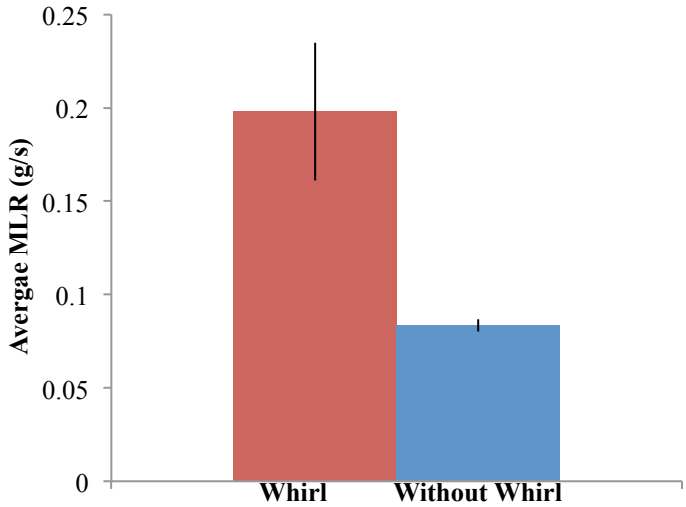

Figure 2.14. Average mass loss rate for 10 mL of heptane.

Figures 2.15 and 2.16 illustrate the mass and average mass loss rate graphs as a function of time and fire whirl implementation. Note the stark difference in burning rate behavior when a fire whirl is introduced.

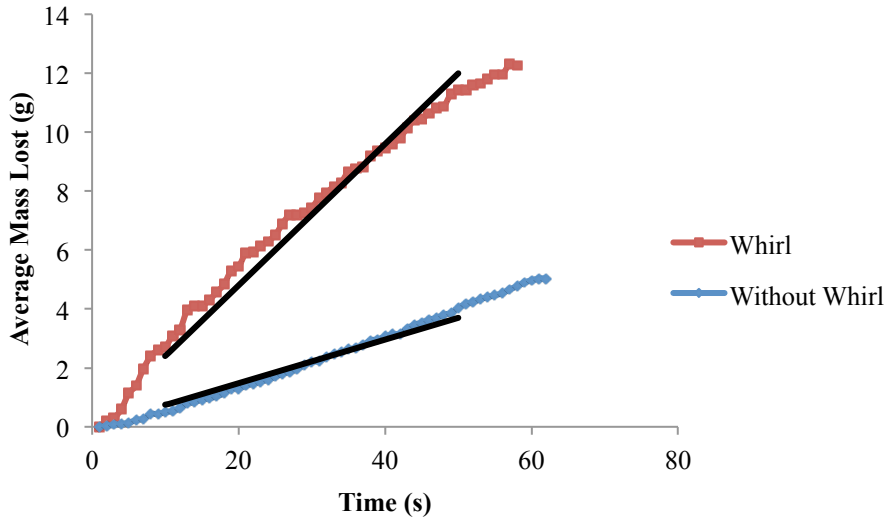

Figure 2.15. Average mass lost as a function of time for 15 mL of heptane. Lines shown represent linear fits to the middle 80% of the averaged data.

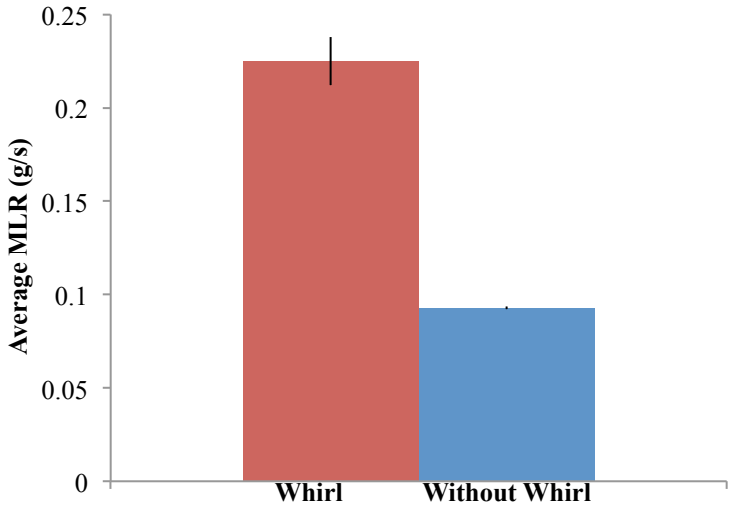

Figure 2.16. Average mass loss rate for 15 mL of heptane.

The plot in Figure 2.17 is a culmination of the previous mass loss rate figures. The average mass loss rate forms a distinct trend for both whirl and non-whirl simulations. It is interesting to see that the slope of the fire whirl trend is greater than that of the non-

whirl simulations. This means that the addition of the whirl has a greater impact on increasing the burning rate of heptane than increasing the volume of fuel available. Error bars were implemented for the without whirl experiments, but are not visible due to data consistency throughout the trials.

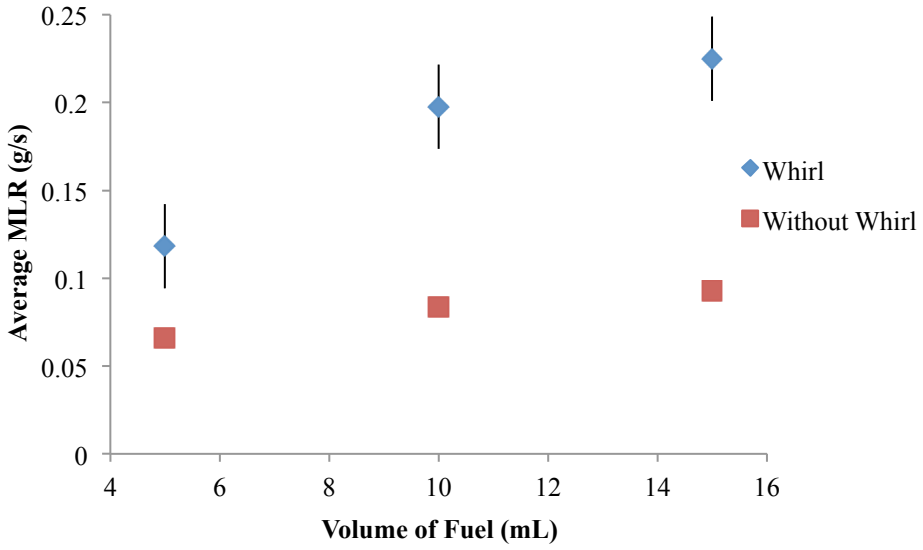

Figure 2.17. Comparison of the average mass loss rates for volumes of heptane as function of fire whirl application.

The plot in Figure 2.18 corresponds to the ratio of the average mass loss rate data represented in Figure 2.17. As can be seen from the trend, there is a positive correlation between the volume of fuel and the effectiveness of the fire whirl. In other words, as the volume of fuel increases, the ratio between the mass loss rates of the whirl and non-whirl experiments increases, indicating that the addition of the fire whirl has a positive impact on the burning rate, at least at the smaller scales studied.

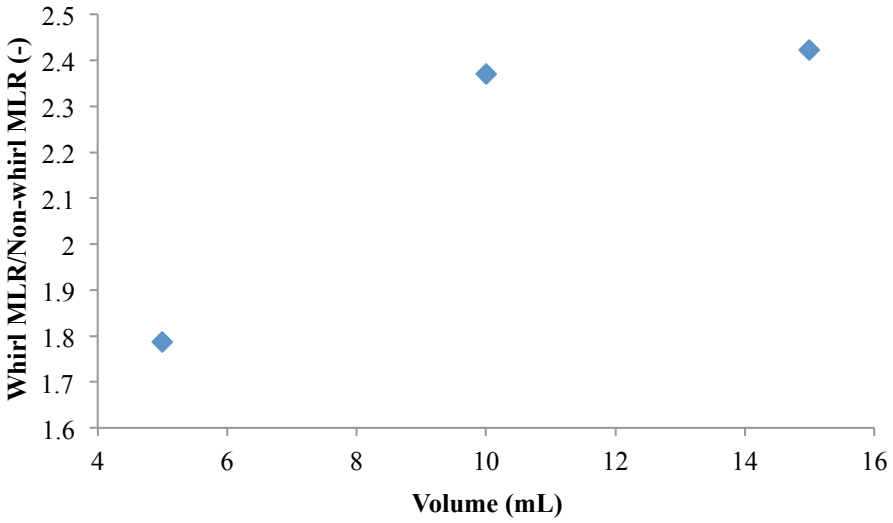

Figure 2.18. Ratio of the average mass loss rates of heptane between whirl and non-whirl configurations.

The plot in Figure 2.19 shows the difference of the mass loss rate values provided in Figure 14. As was the case with Figure 2.18, an increase in fuel volume with the addition of a fire whirl has a positive impact on the mass-burning rate.

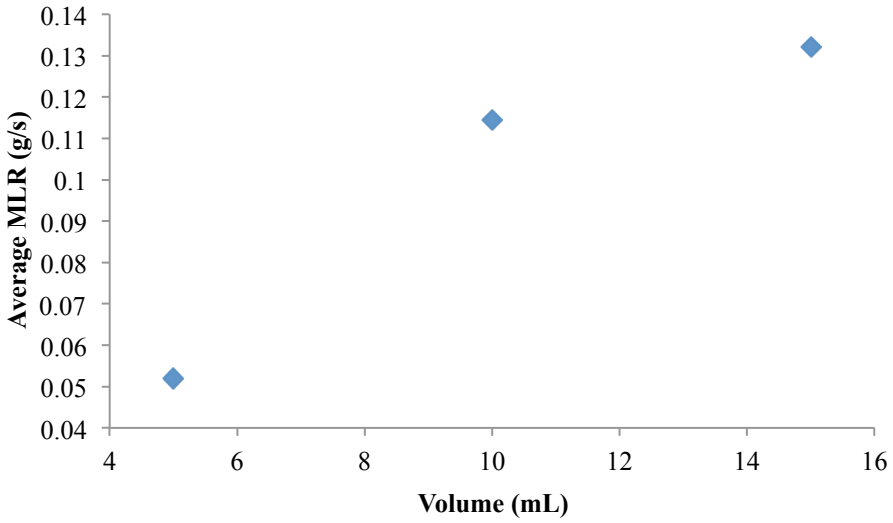

Figure 2.19. Difference in average mass loss rates of heptane between whirl and non-whirl trials.

2.5 Results for Water Circulation

To complete water circulation tests, the setup in Figure 2.1 was employed. The bottom surface aluminum pan containing the fuel/water mixture shown in the figure was hollowed out using a hand-held saw, which allowed water to circulate underneath, simulating the behavior that a liquid fuel spill would experience on a body of water. The metal pan that was originally used as a protective mechanism for the load cell was filled with water and the container was placed on top of the water. This enabled water to flow not only directly underneath of the fuel, but also around the outside of the retaining device, which also replicates the scenario in which liquid fuel spills on an open body of water. Once the container and surrounding pan were filled with water, acetone or heptane was then administered to the container in pre-measured quantities and poured into the

container on top of the water. The fuel was then ignited and mass loss rate data was collected.

These sets of tests were conducted solely using the fire whirl apparatus, as non-whirling results were no longer of interest. This is because fire whirls greatly increase the mass loss rate of a burning fuel, so comparing the results between a fire whirl and a non-fire whirl trial would be redundant. Fire whirl results where therefore compared with and without water circulation only. It is important to note that the height of the water inside of the container was not considered during these experiments, fixed at a specific ullage height, as these tests only concerned the initial impact that water circulation had on mass loss rate. The effect that this height and resulting circulation had on the burning rate is addressed later in Chapter 3.

Figures 2.20 through 2.23 illustrate the effect that water circulation has on the mass loss rate. For acetone, implementing water circulation via removal of the base of the fuel pan provides a mass-burning rate that is about 30% greater than that of the standard fire whirl setup without water circulation. In the case of heptane, allowing the water to circulate in the experimental setup provides a similar increase in the mass loss rate. The 15-mL heptane trial saw an increase of about 30%, but the mass loss rate for the 10-mL experiment was upwards of 37%. It is important to note that the water circulates in the same direction as the fire whirl. Bulk motion induced by shear between incoming air and the liquid surface is believed to be the reason why the efficacy of the fire whirl increased.

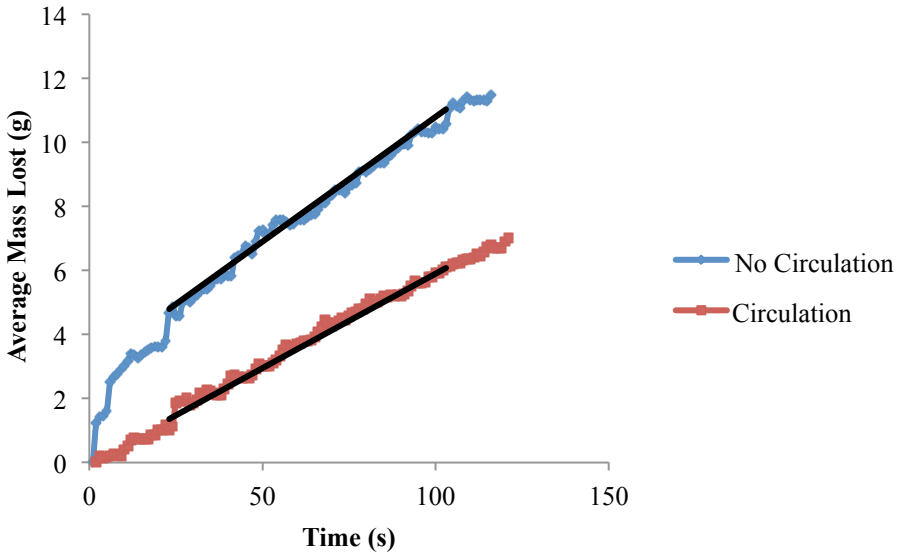

Figure 2.20. Average mass lost for fire whirl trials with and without water circulation for 10 mL of acetone. Lines shown represent linear fits to the middle 80% of the averaged data.

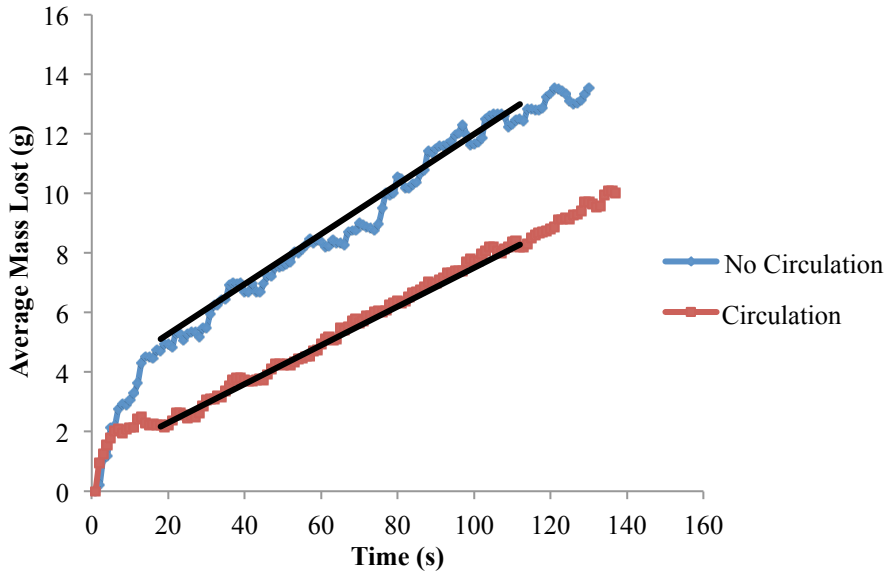

Figure 2.21. Average mass lost for fire whirl trials with and without water circulation for 15 mL of acetone. Lines shown represent linear fits to the middle 80% of the averaged data.

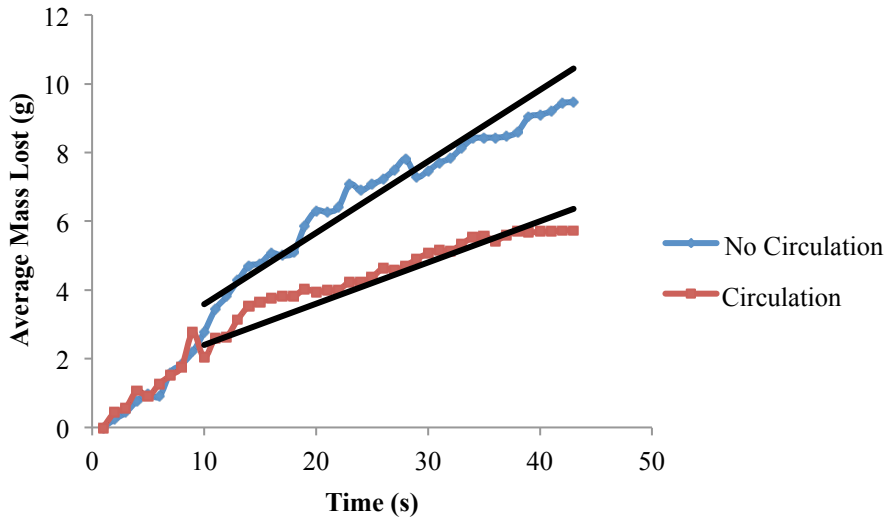

Figure 2.22. Average mass lost for fire whirl trials with and without water circulation for 10 mL of heptane. Lines shown represent linear fits to the middle 80% of the averaged data.

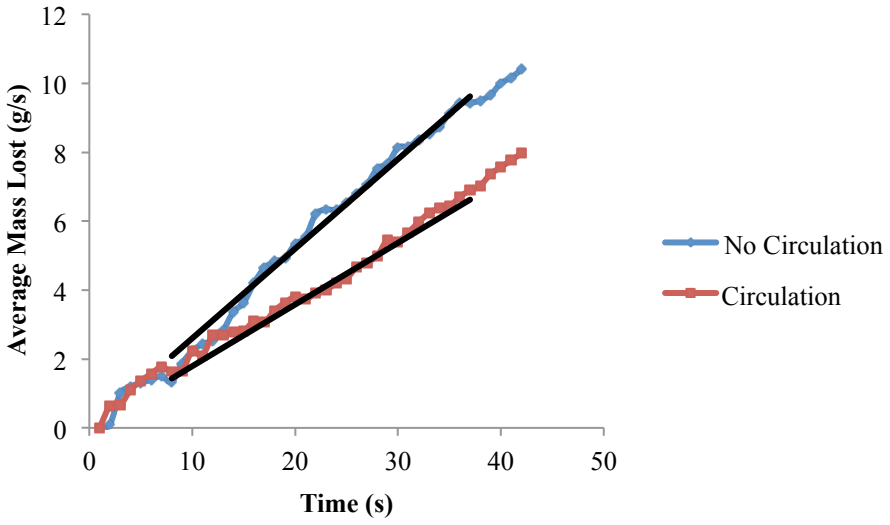

Figure 2.23. Average mass lost for fire whirl trials with and without water circulation for 15 mL of heptane. Lines shown represent linear fits to the middle 80% of the averaged data.

Figures 2.24 and 2.25 provide the average mass loss rate as a function of fuel volume and water flow circulation. As can be seen from the figure, the difference between the two mass loss rates varies minimally as a function of fuel volume. There is only a slight increase in burning rate as the volume is increased, but nowhere near as significant as in the case with heptane. As was mentioned previously, this stems from the fact that acetone has a lower heat of combustion and is also much less sooty meaning that there is reduced radiative heat feedback to the surface and this a lower heat-release rate at the fire. Coupling these factors results in a less significant growth in burning rate as is illustrated in Figures 2.21 and 2.22, the former corresponding to acetone and the latter to heptane.

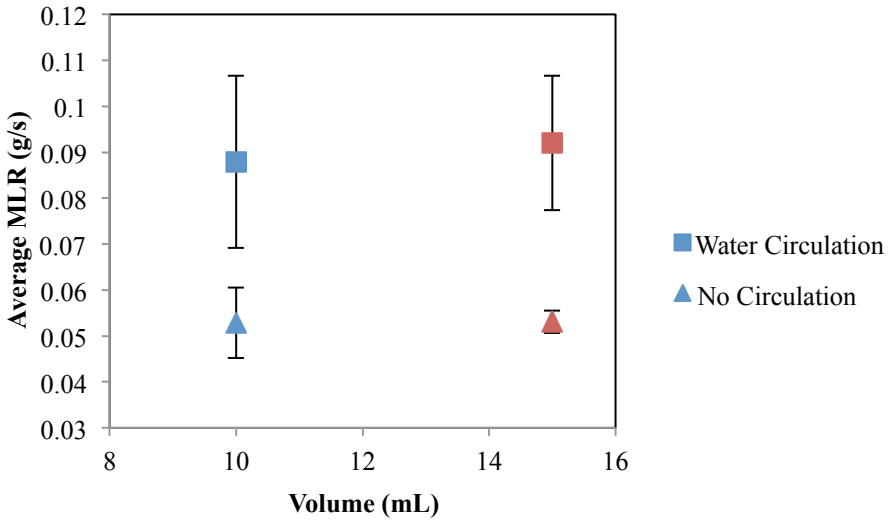

Figure 2.24. Average mass loss rate as a function of volume with water circulation for acetone with a fire whirl.

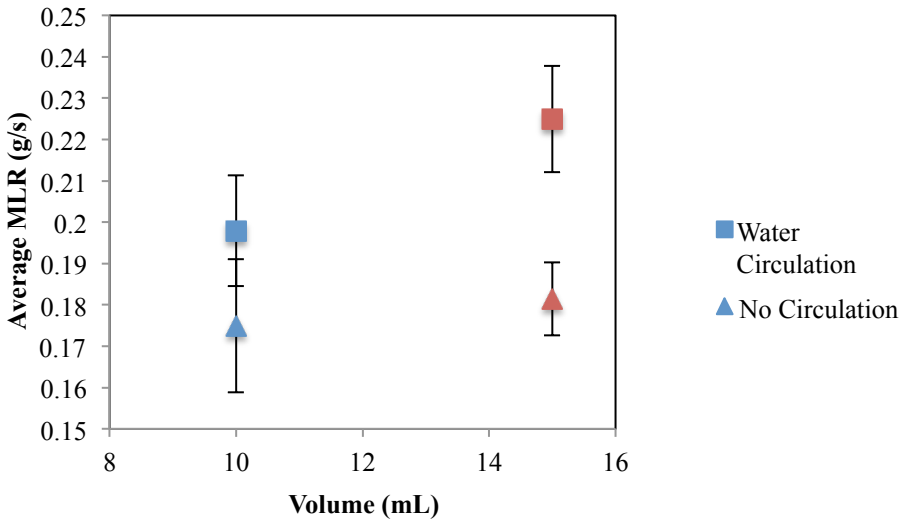

Figure 2.25. Average mass loss rate as a function of volume with water circulation for heptane with a fire whirl.

Chapter 3: Effects of Varying Container Size and Ullage Height

The second set of tests varied two additional parameters – the fuel container size and the ullage height of the fuel. The ullage height is the distance between the top of the container and the height of the fuel/water mixture. Figure 3.1 provides an illustration of this measurement.

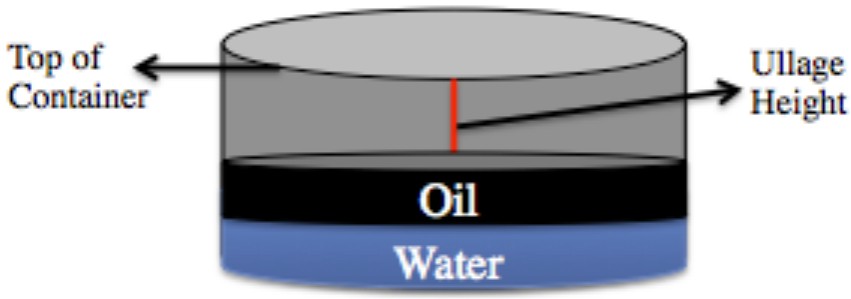

Figure 3.1. Illustration of ullage height in fuel container.

The ullage height was varied in the experiments because it has been previously shown to affect the mass burning rate and ignition and extinction conditions for hydrocarbon fuels floating over water. Increasing this height meant reducing the fuel/water mixture height, which is believed to induce edge effects, limiting the amount of oxygen that would be in contact with the liquid fuel, subsequently reducing the mass loss rate. This occurs because the air has to physically penetrate the threshold that is the top of the container and then descend overtop of the fuel vapor, which reduces the amount of total oxygen that can come in contact with the fuel.

The two containers that were used measured 9 cm and 24 cm in diameter. The small container can be seen in Figure 3.2 and the large one in Figure 3.3.

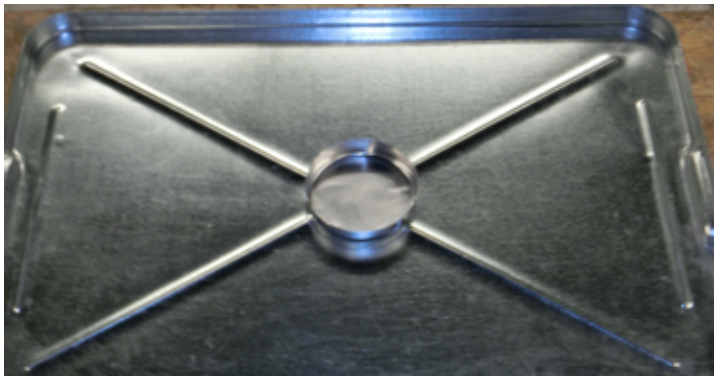

Figure 3.2. Small fuel container (9-cm diameter) with protective pan.

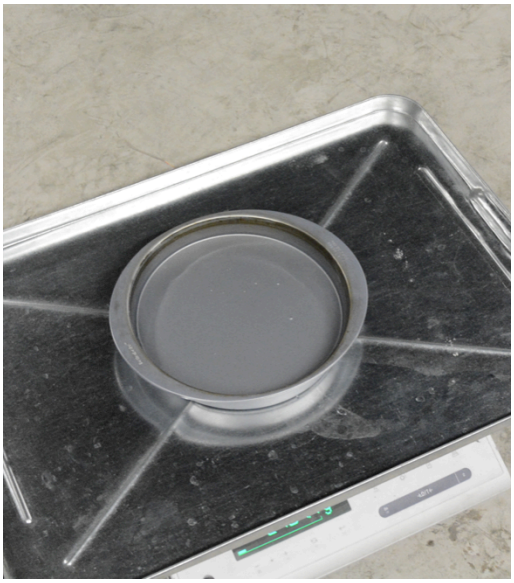

Figure 3.3. Large fuel container (24-cm diameter) with protective pan and load cell.

It is important to note that water circulation was not allowed in these experiments, because the goal of these tests was to evaluate how the ullage height impacted the mass-burning rate. Directly limiting additional variables (such as water circulation) ensured that the only varying factor was the liquid fuel/water interface height. Heptane fuel was

used for these tests because it provided more distinct mass loss rate comparisons, which could help to better identify whether ullage height measurements impact mass loss rate behavior when a fire whirl is induced in comparison to normal pool fire behavior. Another important component of the ullage height is that it refers to the initial depth of the oil. Water was not added into the bottom of the container during testing to supplement the vaporizing fuel, so the actual ullage height reduced during burning. In the following graphs, two terms will be used: minimum ullage height and a numerically defined height. A minimum ullage height corresponds to a water/liquid fuel interface at the top of the container, which minimizes the impact of lip effects. The numerically defined ullage height reflects a water/liquid fuel interface at a specific distance measured from the bottom of the container.

3.1 Results with Small Container

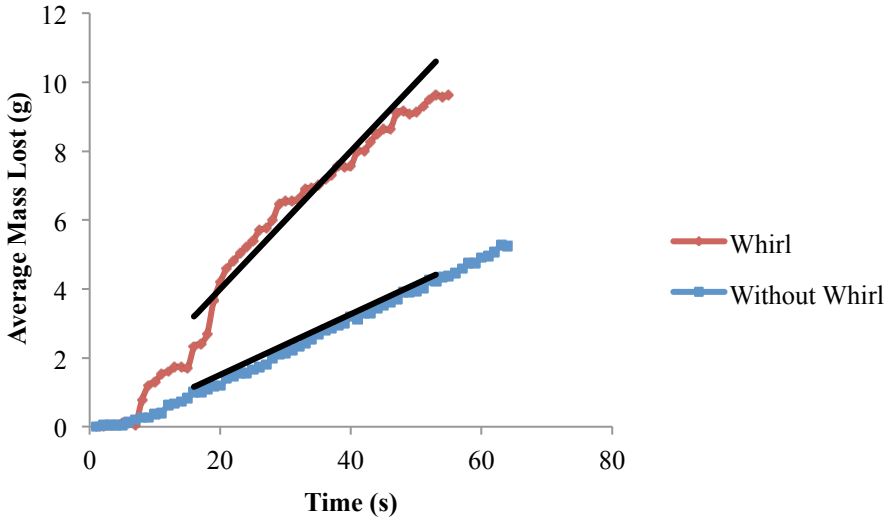

Figure 3.4. Small container – average mass lost for 10 mL of heptane with a 0.5-cm ullage height. Lines shown represent linear fits to the middle 80% of the averaged data.

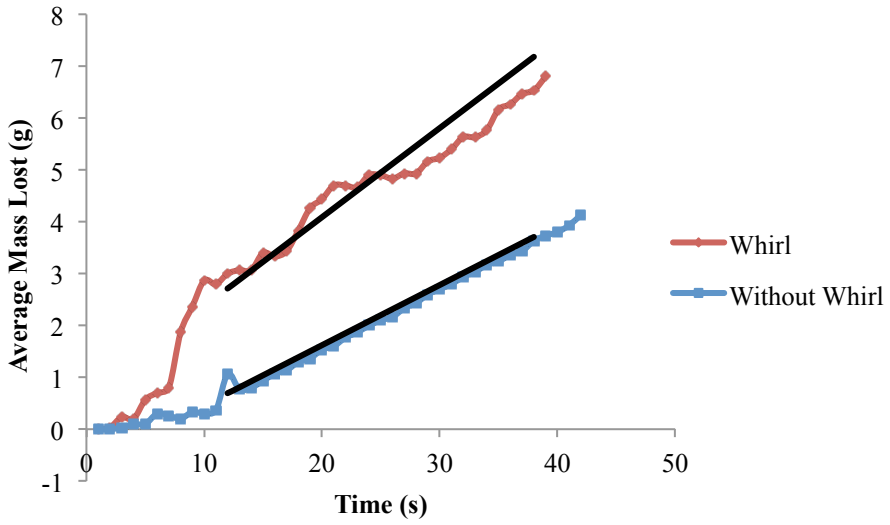

Figure 3.5. Small container – average mass lost for 10 mL of heptane with a minimum ullage height. Lines shown represent linear fits to the middle 80% of the averaged data.

Figure 3.6 provides a comparison between the two fire whirls as a function of ullage height. As can be seen from the figure, the scenario where the liquid fuel/water interface height is 0.5 cm below the lip of the container generated a mass loss rate that is about 15% larger than was the case with a minimal ullage height (interface at the top of the container). This is the opposite of what was predicted, and indicates that 0.5 cm isn't enough of a height differential to compromise the burning rate of the fuel. In order to evaluate the impact ullage height had on burning rate more thoroughly, the ullage height was substantially increased for subsequent testing as is noted in Section 3.2.

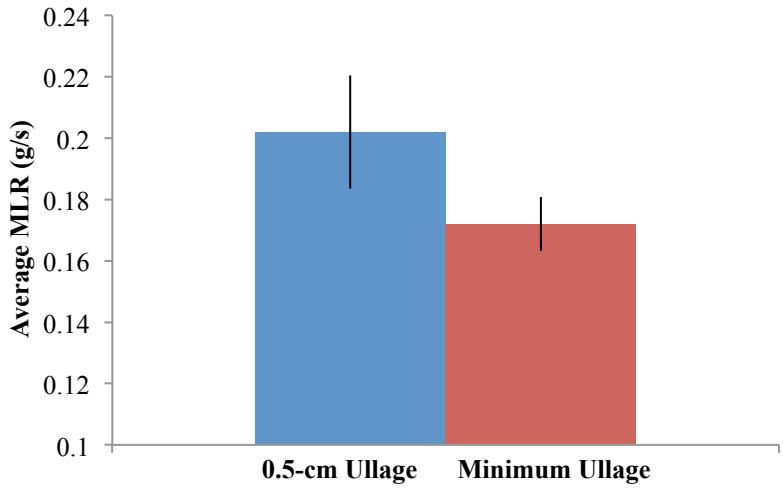

Figure 3.6. Average mass loss rate per unit time as a function of fire whirl and ullage height for 10 mL of fuel.

The same procedure was employed for the 15-mL experiments to evaluate the effects that increasing the volume of fuel had in conjunction with varying the ullage height. The results are shown in Figures 3.7 and 3.8. Figure 3.9 illustrates that there is only a small difference as a function of ullage height, meaning that for a container of this size, there isn't an appreciable difference in mass loss rate. This is due to the fact that the container isn't deep enough to influence the heat transfer between the flame and the unburned fuel when the liquid fuel/water interface is only 0.5 centimeters from the bottom of the container.

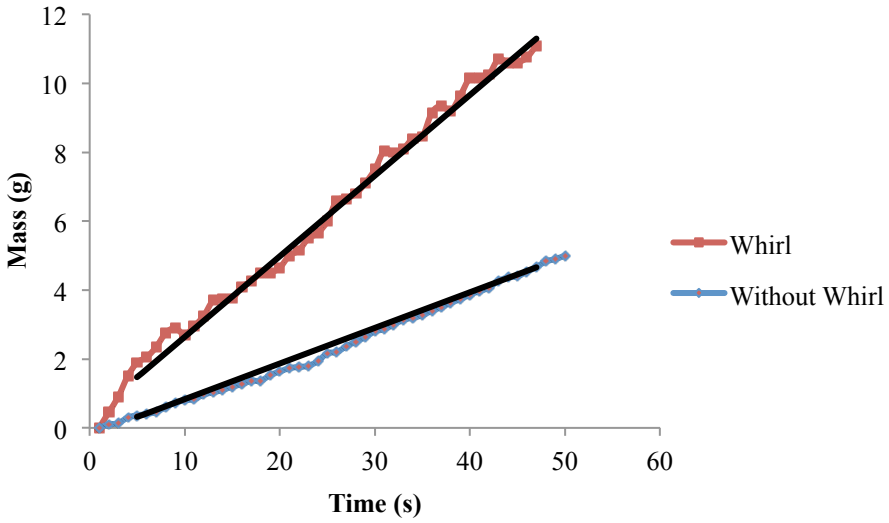

Figure 3.7. Small container – average mass lost for 15 mL of heptane with a 0.5-cm ullage height. Lines shown represent linear fits to the middle 80% of the averaged data.

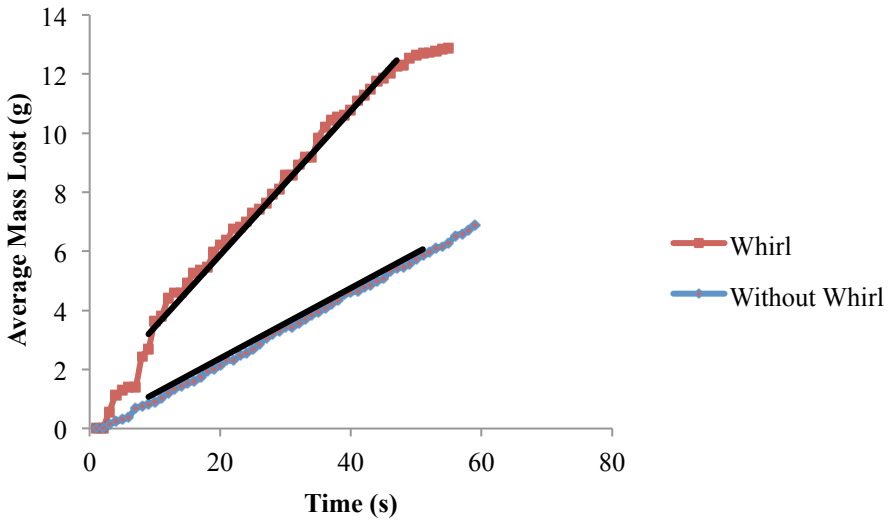

Figure 3.8. Small container – average mass lost for 15 mL of heptane with a minimum ullage height. Lines shown represent linear fits to the middle 80% of the averaged data.

The lines superimposed overtop of the plots represent the range of data that was used to evaluate the average mass loss rate. The bar graphs in Figure 3.9 correspond to the whirl data provided in the previous two figures. The difference between the two values is negligible as the data for minimum ullage mass loss rate experiment is only 4% less than that of the stemming from the 0.5-cm ullage height.

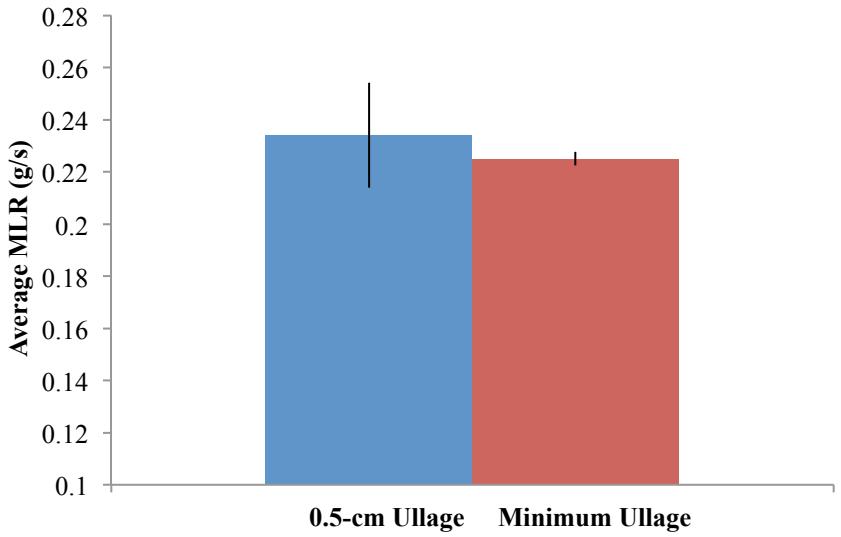

Figure 3.9. Average mass loss rate per unit time as a function of fire whirl and ullage height for 15 mL of fuel.

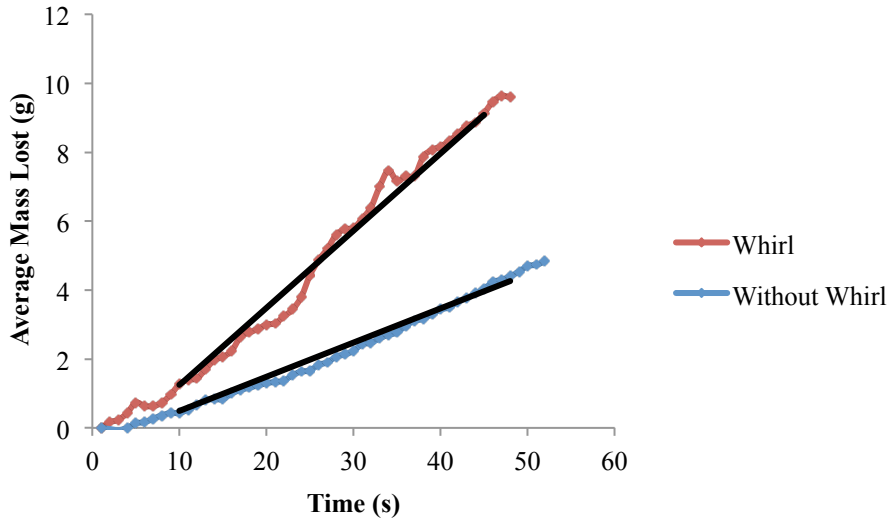

Figure 3.10. Small container – average mass lost for 20 mL of heptane with a 0.5-cm ullage height. Lines shown represent linear fits to the middle 80% of the averaged data.

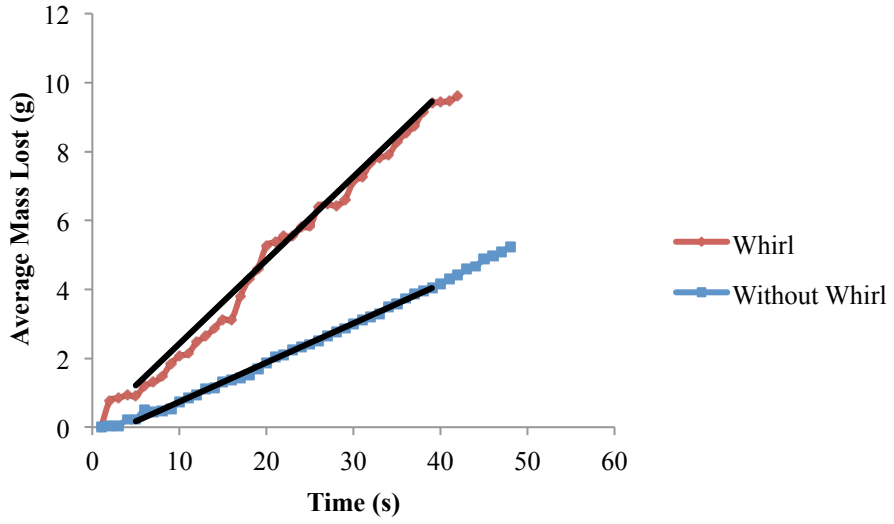

Figure 3.11. Small container – average mass lost for 20 mL of heptane with a minimum ullage height. Lines shown represent linear fits to the middle 80% of the averaged data.

The lines superimposed overtop of the plots represent the range of data that was used to evaluate the average mass loss rate. Figure 3.12 provides an illustration of the mass loss rate behavior that was inconsistent with the 10- and 15-mL trials in that fire whirl for the "minimum ullage" set up produced a greater mass loss rate than what was found for the 0.5-cm ullage. When the lip effects are minimized, the rate at which the fuel burns is increased due to more consistent airflow. This is the opposite of what is provided in Figure 3.6 in which case the ullage height actually had a positive effect on the mass loss rate. This means that the volume of fuel has a greater impact on the burning rate than the ullage height. This was critical information, and ultimately defined the experimental setup for crude oil testing. It is important to note that lips will not form during an *in situ* burn, but it was necessary to evaluate the impact that ullage height had on mass-burning rate as a way to develop repeatability and precision data collection during experimentation.

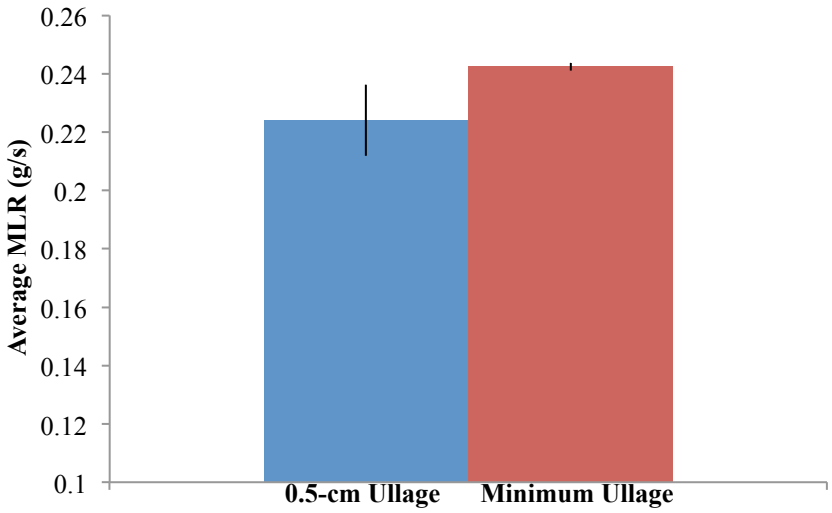

Figure 3.12. Average mass per unit time as a function of fire whirl and ullage height for 20 mL of fuel.

3.2 Results with a Larger Container

After testing with the 9-cm diameter fuel container, a larger 24-cm diameter pool was used to evaluate whether the ullage height has an effect on the mass loss rate for larger pools. This setup is provided in Figure 3.3. Figure 3.13 is a snapshot of a fire whirl developed in the larger container.

Figure 3.13. Developed fire whirl in a 24-cm diameter container.

As was done for the smaller container, a predetermined ullage height and fuel volume was tested with and without a fire whirl. The resultant whirl data was then compared to demonstrate the effect that ullage height has on the mass loss rate.

Figures 3.14 and 3.15 provide the mass vs. time curves for 10 mL of heptane poured into a 24-cm container at 1.5-cm and minimal ullage heights. The reason that the ullage height was increased from 0.5 to 1.5 cm was two fold: first, the results that were found using the smaller container proved inconclusive – possibly due to the fact that container was not deep enough – as a judgment could not be made stating whether ullage height had an impact on the mass loss rate. Second, the larger pan has much more depth, ultimately

allowing for testing to be completed at a greater ullage height, which would help to better distinguish whether the ullage height affects the mass loss rate.

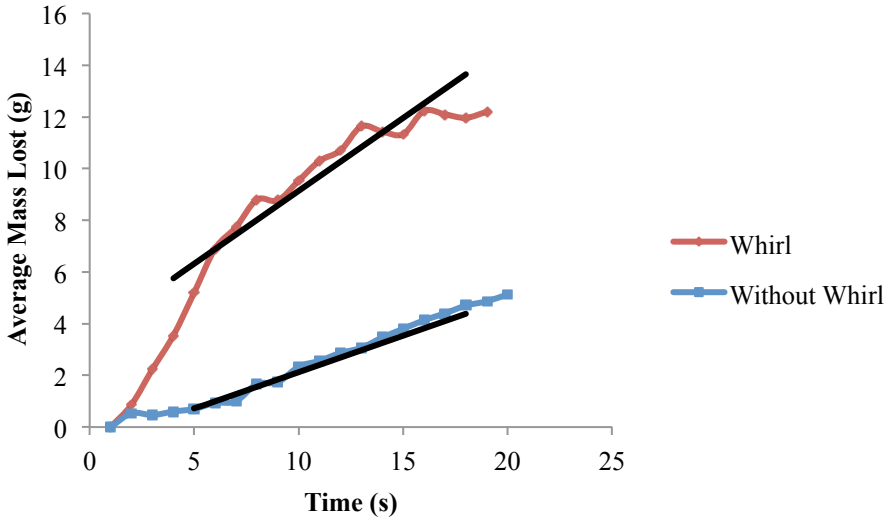

Figure 3.14. Large container – average mass lost for 10 mL of heptane with a 1.5-cm ullage height. Lines shown represent linear fits to the middle 80% of the averaged data.

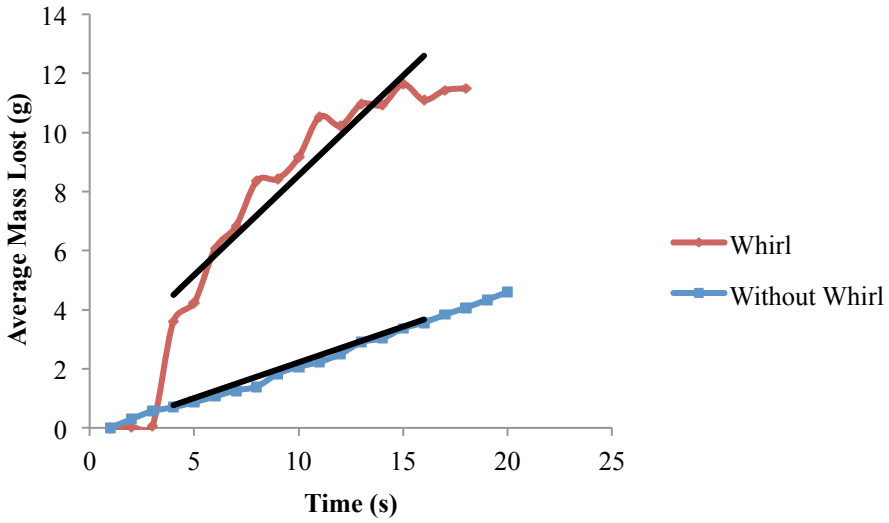

Figure 3.15. Large container – average mass lost for 10 mL of heptane with a minimum ullage height. Lines shown represent linear fits to the middle 80% of the averaged data.

Figure 3.16 is a comparison between the fire whirl data at for heptane at each ullage height. As can be seen from the figure, the ullage height has only a marginal effect on the mass loss rate. This may be attributed to the fact that the time required to completely burn the fuel is quite small due to the small volume, so there may not be enough time for the edge effects to actually make an impact.

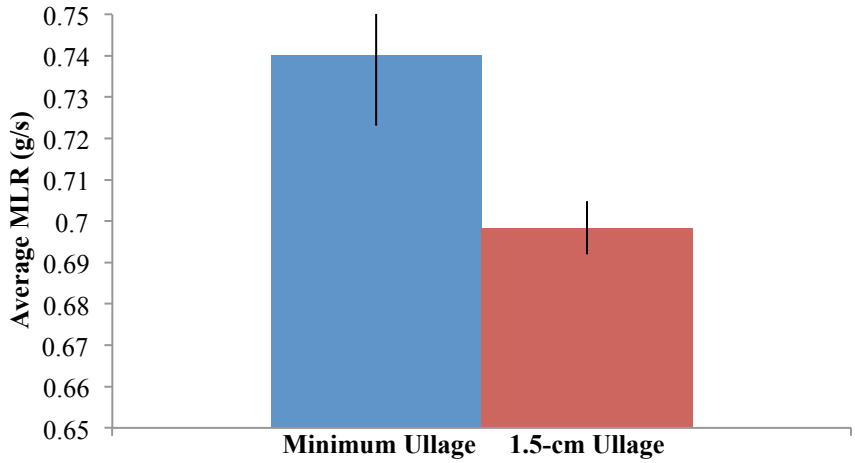

Figure 3.16. Average mass per unit time as a function of fire whirl and ullage height for 10 mL of heptane.

Figures 3.17 and 3.18 provide results with the same test setup that was employed for the data in Figures 3.14 and 3.15 with the only difference being the volume of fuel used (15 mL). As can be seen from the figures, there is a noticeable difference in the mass loss rate with the addition of a fire whirl. This differential is even more pronounced when the ullage height is minimized, which has a major implication: the ullage height has a much greater impact on the mass loss rate of heptane when a fire whirl is introduced then for a basic pool fire experiment.

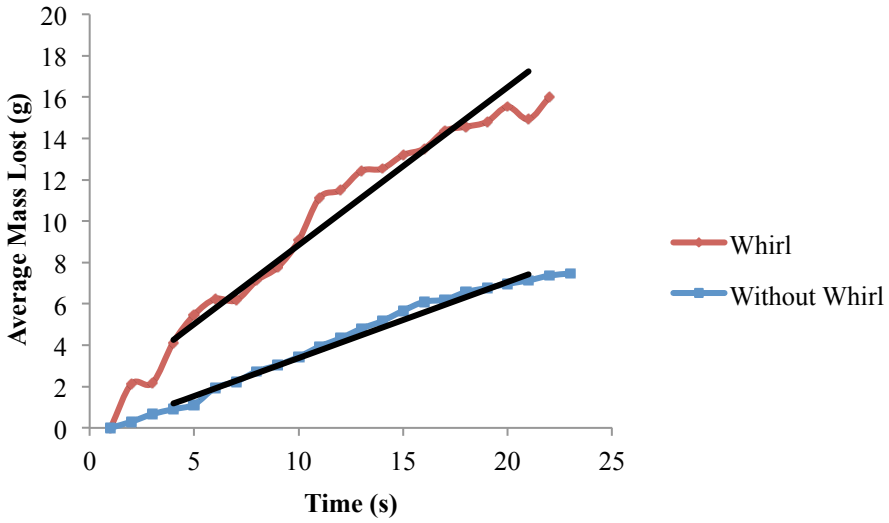

Figure 3.17. Large container – average mass lost for 15 mL of heptane with a 1.5-cm ullage. Lines shown represent linear fits to the middle 80% of the averaged data.

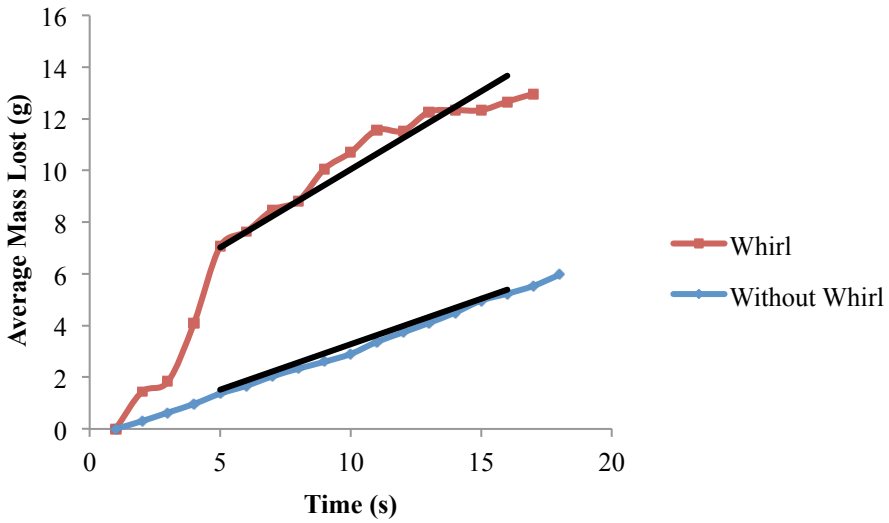

Figure 3.18. Large container – average mass lost for 15 mL of heptane with a minimum ullage height. Lines shown represent linear fits to the middle 80% of the averaged data.

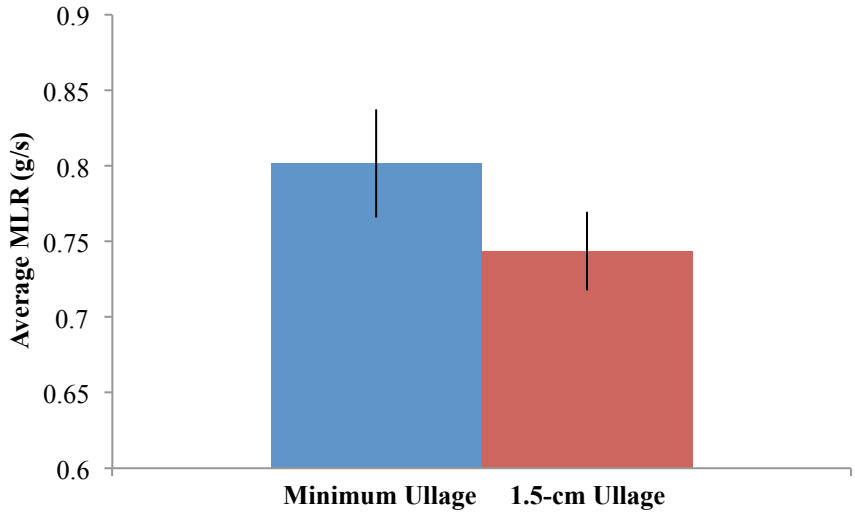

Figure 3.19. Average mass per unit time as a function of fire whirl and ullage height for 15 mL of heptane.

The last set of tests performed evaluate the influence that ullage height had on mass burning rate data used 20 mL of heptane. Figures 3.20 and 3.21 provide the data for both 1.5-cm ullage and minimum ullage heights, respectively.

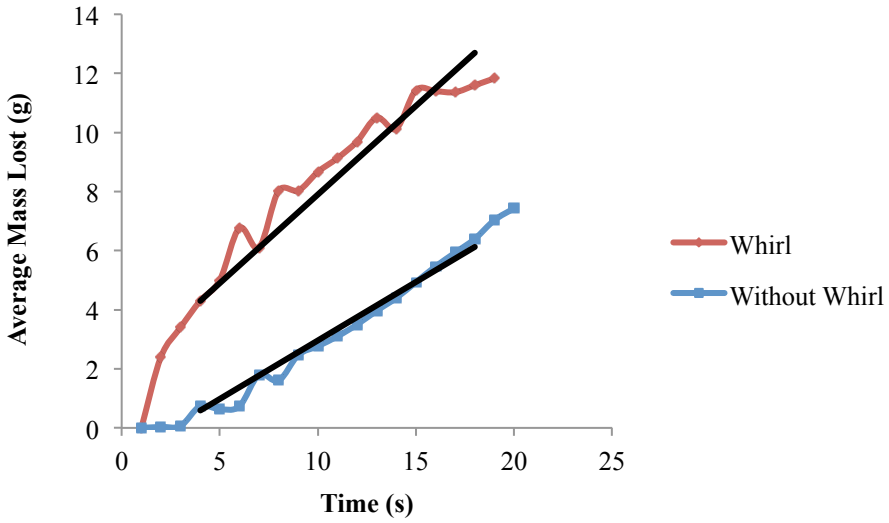

Figure 3.20. Large container – average mass lost for 20 mL of heptane with a 1.5-cm ullage height. Lines shown represent linear fits to the middle 80% of the averaged data.

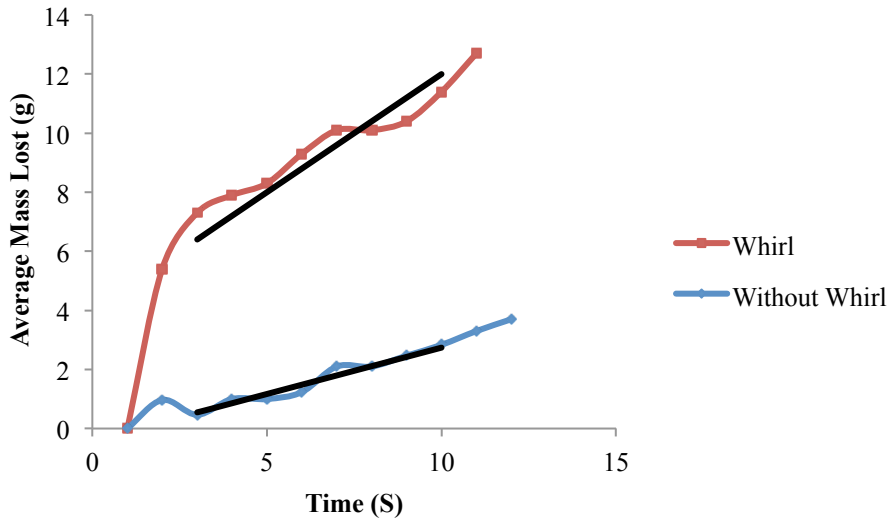

Figure 3.21. Large container – average mass lost for 20 mL of heptane with a minimum ullage height. Lines shown represent linear fits to the middle 80% of the averaged data.

The lines superimposed overtop of the plots represent the range of data that was used to evaluate the average mass loss rate. Figure 3.22 is a culmination of the fire whirl results from Figures 3.20 and 3.21. Similar to the 10 and 15 mL experiments, the 20 mL results also show that the mass loss rate is greater in situations where the ullage height is at a minimum (the liquid fuel/water interface is positioned at the lip of the container).

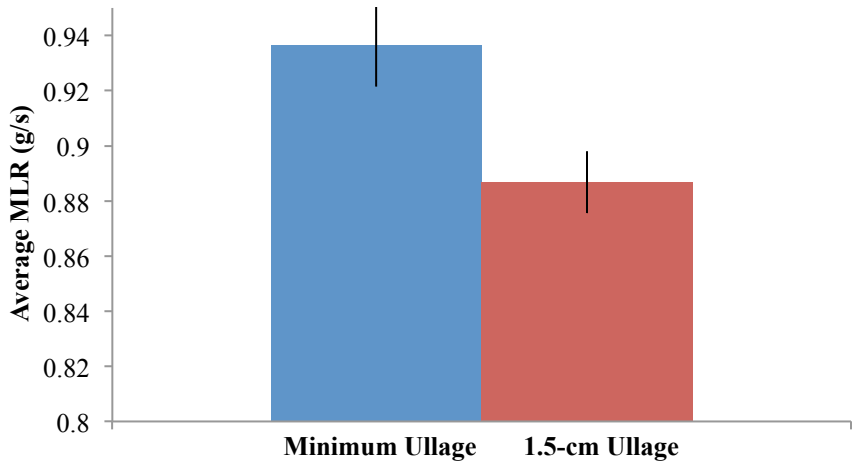

Figure 3.22. Average mass loss rate per unit time as a function of fire whirl and ullage height for 20 mL of heptane.

In short, the ullage height has a noticeable impact on the rate at which fuel burns, even more pronounced with the addition of a fire whirl. This helped to finalize the parameters that would be tested with crude oil, the focal point of this effort. Minimizing the ullage height to mitigate heat transfer effects and maximizing the volume of fuel to increase the burning rate were important factors that were discovered through the research conducted with heptane and acetone, and subsequently implemented in crude oil burning trials.

Chapter 4: Testing with Crude Oil

Only after finalizing the experimental procedure with acetone and heptane was crude oil tested experimentally.

Unfortunately experimenting with crude oil in an open water environment, as was done for heptane, could not be accomplished for several reasons. First, steel was used rather than aluminum as the containing vessel for crude oil because the aluminum melted when exposed to the flames produced by the oil. Also, the steel was unable to be hollowed out for experimental testing due to time and budget constraints, so water was unable to circulate underneath the fuel. Through the research conducted it was found that water circulation has an appreciable effect on the mass loss rate, but testing this theory with crude oil will be incorporated in later work.

The procedure for collecting mass loss rate data was nearly identical to what was done for the acetone and heptane experiments with the only difference being the way in which the fuel was ignited. For the acetone and heptane scenarios, a lighter was used as the ignition catalyst, while crude oil required extended heating by a propane blowtorch. A blowtorch had to be used because it provided the heat necessary to raise the top layer of the oil to its flashpoint temperature.

The first set of trials proved inaccurate and produced unrepeatable data because of a phenomenon known as boil-over. Boil-over occurs when the water underneath the fuel reaches its boiling point temperature – 100 degrees Celsius – while a flame is still active

on the surface [38-41]. The water begins to vaporize, which forms small steam bubbles that thrust upward, penetrating the surface of the water/fuel mixture at a rapid velocity. This forces water and crude oil out of the container and into the air and surrounding area, ultimately making accurate mass loss rate calculations impossible. Figure 4.1 shows the initial setup used. It should be noted that instead of using a plywood sheet as a heat sink, three flame retardant ceramic sheets were positioned between the load cell and the metal pan, which was a more effective and less obtrusive way of protecting the device.

Figure 4.1. Initial crude oil testing setup.

To rectify the boil-over issue, the container in which the crude oil was located was placed in a large steel cylinder filled with water. The pan provided a cooling effect that helped prevent boil-over from occurring and also simulate the cooling effect water would have in real in-situ burning applications on open water. This cooling effect can be attributed to the thermal capacity of water and a high specific heat, which absorbs a fair amount of heat during the steady burning stage. The specific heat of water is considerable, meaning that a large amount of energy is required to increase a unit mass of water. One of the benefits of supplementing the experiment with an additional container is that it provided

circulatory water motion, which helped to simulate a fuel spill on a body of water. While the fuel was not able to move freely on top of the water, as would be the case in an ocean environment, it was able to experience circulating water flow along the exterior of the container, which helps simulate a convective cooling effect that would be present.

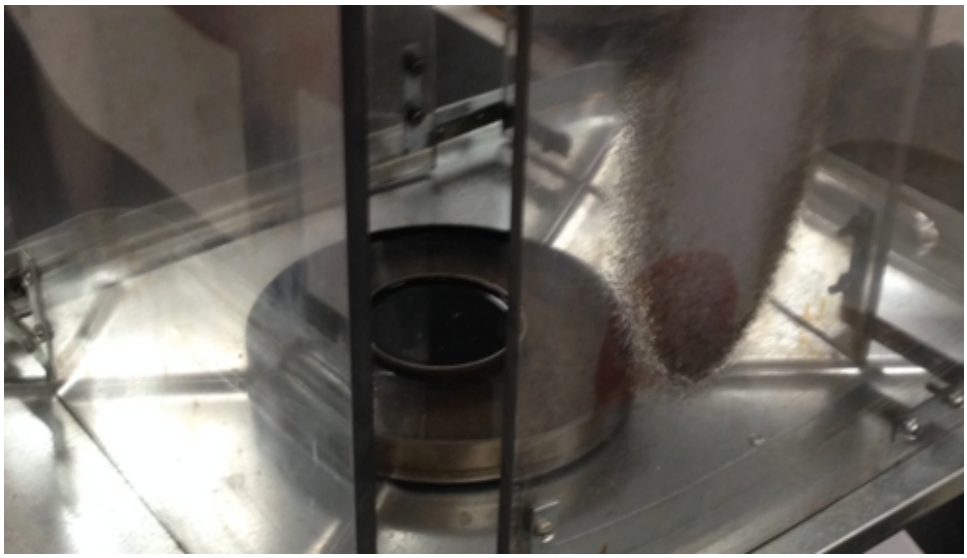

Figure 4.2. Updated setup with section of fire whirl apparatus.

Once the additional pan was administered, water was added to both the fuel and protective containers. A specific quantity of crude oil – 15, 20, 25, or 30 mL – was then poured on top of the water. It is important to note that the amount of water varied between the four crude oil volumes. As the crude oil volume increases, the amount of water necessary to fill the container decreases. To compensate for this, the volume of water that was necessary to complete the 15 mL crude oil trials was reduced by five, 10, and 15 mL for the 20, 25, and 30 mL experiments, respectively. Once the correct water and fuel totals were added, the crude oil was ignited and data collection could begin. The mass loss rate collection process was the same method that was used for the acetone and heptane trials: initiate the load cell program, ignite the fuel, and stop the program once

the fire burns out. Two additional analysis methods were introduced for the crude oil experiments – soot collection and residual fuel measurements. The purpose of the former was to evaluate the soot produced during crude oil combustion and to determine if the implementation of a fire whirl would ultimately affect this production. The residual fuel measurements were completed to see if adding a fire whirl to the experiment would alter the total mass of crude oil consumed during the burn. Both of these factors would help to support the theory that the addition of a fire whirl is an effective means to increase the efficiency of in-situ burning.

To find these values, 3M hydrophobic oil-absorption pads were used. For soot collection, a pad was cut to the size of the fume hood vent, weighed, and then placed over the exhaust vent, trapping any soot particulates that were generated by the fire. The fuel was ignited, and once the test concluded, the pad was removed from the vent hood and weighed again. This process was repeated for every trial, both with and without the fire whirl generator. Traditional filter paper was also tested, however not enough soot was collected on these pads to be measureable. The oil absorption pads appear to collect soot to a measureable level, so therefore at least a comparable analysis could be completed. Future work will include specifically identified filters to more accurately quantify soot.

For the residual fuel analysis, a 3M-absorption pad was cut to the size of the small pool containing the fuel and weighed. Once the test was completed, the pad was draped over the top of the pool and lightly depressed until the remaining fuel residue was collected. The pads were then dried to allow whatever water accumulated – the pads are not 100%

hydrophobic – to evaporate. The pads were then weighed again to measure how much of the fuel and solid product was remaining. This process was repeated for every trial, both with and without the fire whirl generator.

4.1 Results with Crude Oil

As was the case with the acetone and heptane scenarios, there is an appreciable difference between the mass loss rates of the whirl and non-whirl experiments for crude oil. The subsequent figures illustrate this.

In figures 4.3 through 4.10, mass lost and mass loss rate plots for varying volumes of crude oil ranging from 15 to 30 mL are plotted. The general trend mirrors that of heptane and acetone - as the volume of fuel increases, so too does the mass loss rate. This is an important distinction because a fuel spill on a body of water will be substantially larger in size and volume than the tests conducted in the laboratory, so there is a possibility that the effectiveness of a fire whirl may be even more prominent.

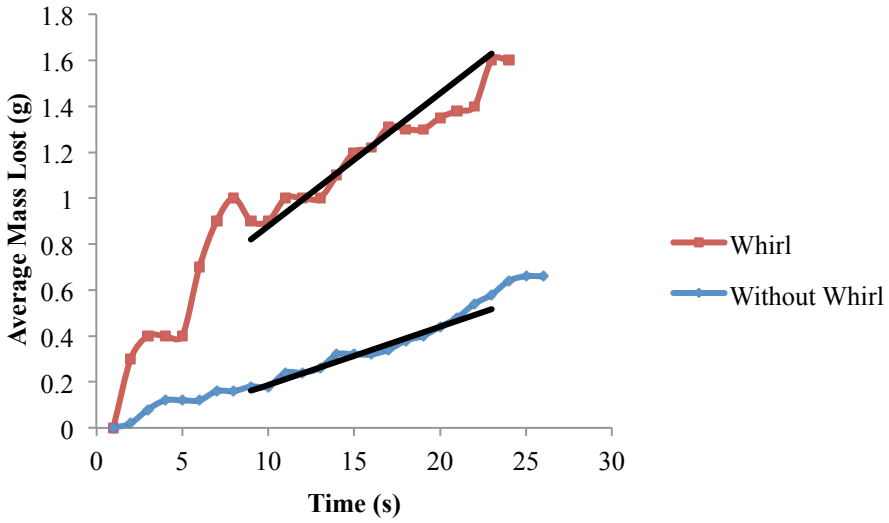

Figure 4.3. Average mass lost for 15 mL of crude oil. Lines shown represent linear fits to the middle 80% of the averaged data.

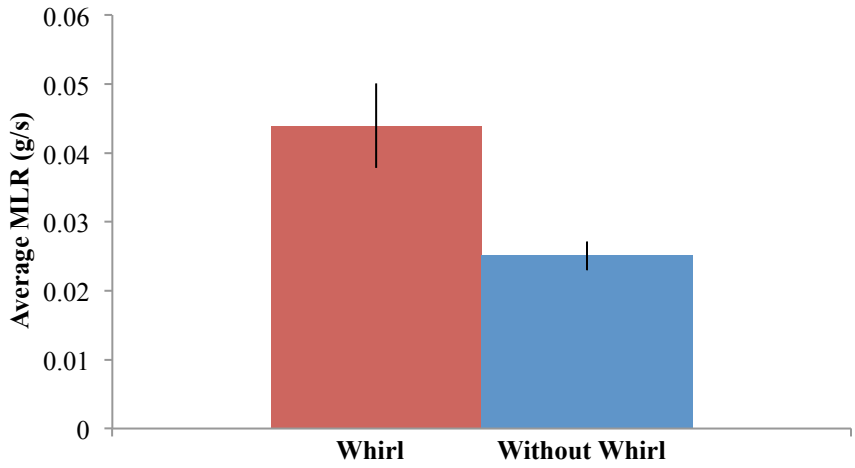

Figure 4.4. Average mass loss rate for 15 mL of crude oil.

The same technique that was employed for the 15 mL testing was used for the 20, 25, and 30 mL testing, with the only difference being the slight reduction in water necessary to fill the container to the top.

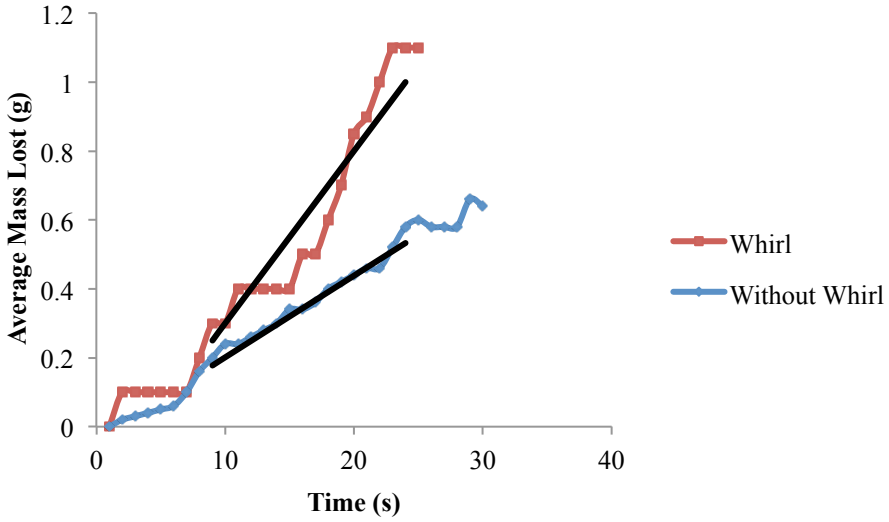

Figure 4.5. Average mass lost for 20 mL of crude oil. Lines shown represent linear fits to the middle 80% of the averaged data.

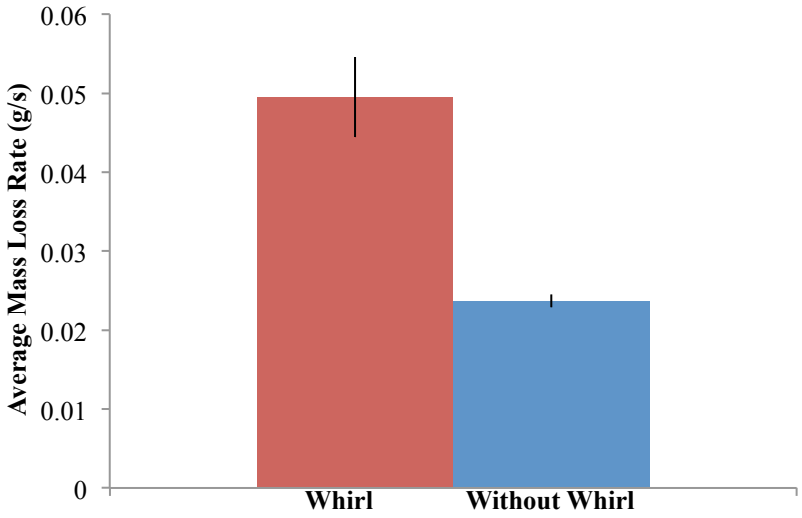

Figure 4.6. Average mass loss rate for 20 mL of crude oil.

As can be seen from Figure 4.6, the difference in mass loss rate between the two experiments is noticeably larger than the data reported for the 15 mL trial in Figure 4.4. The reason this occurs is due to the thickness of the crude oil. When the oil is poured on top of the water, an inherent thickness will develop. The top of the oil will ignite once exposed to a blowtorch, while the oil underneath acts as insulation from the cool water below. The thickness of the oil recedes with time, and eventually becomes too thin to the point that heat from the fire transfers from the oil to the water, which drops the surface temperature of the oil below the required ignition temperature, subsequently extinguishing the flame [4]. Because of this, increasing the fuel depth increased the amount of insulation and the amount of fuel that is consumed, which is why the 20 mL trial produced a higher burning rate. This same trend persists for the 25 and 30 mL experiments, as can be seen in Figure 4.8 and 4.10 and in summation in Figure 4.11.

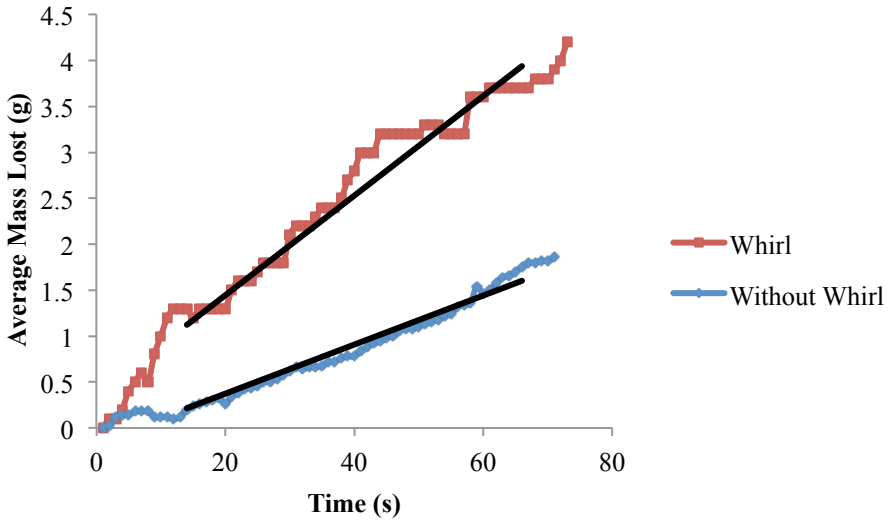

Figure 4.7. Average mass lost for 25 mL of crude oil. Lines shown represent linear fits to the middle 80% of the averaged data.

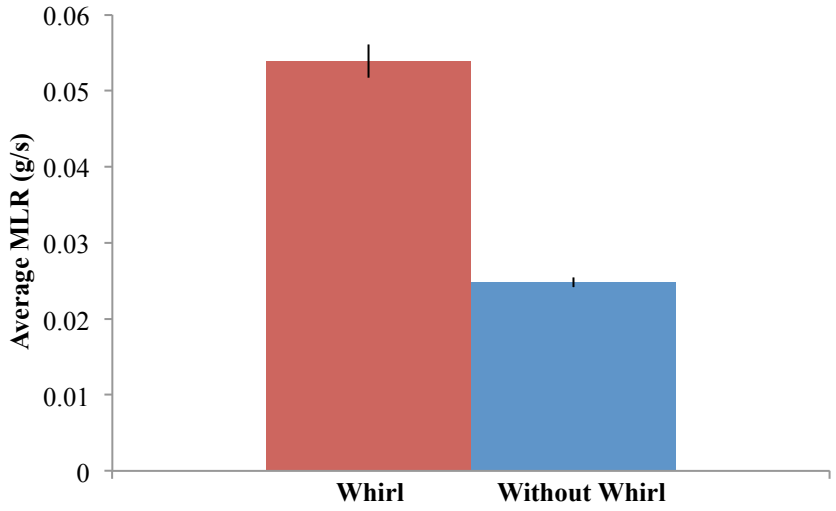

Figure 4.8. Average mass loss rate for 25 mL of crude oil.

Figures 4.9 and 4.10 correspond to the average mass loss rate plots for 30 mL of crude oil. It is hard to distinguish the differences in value between the 30 mL trials and the other experiments (15, 20, and 25 mL) through the graphs because the values are similar in nature, but it should be noted that there is a distinct trend that is developed as the volume of fuel is increased. Figure 4.11 demonstrates this.

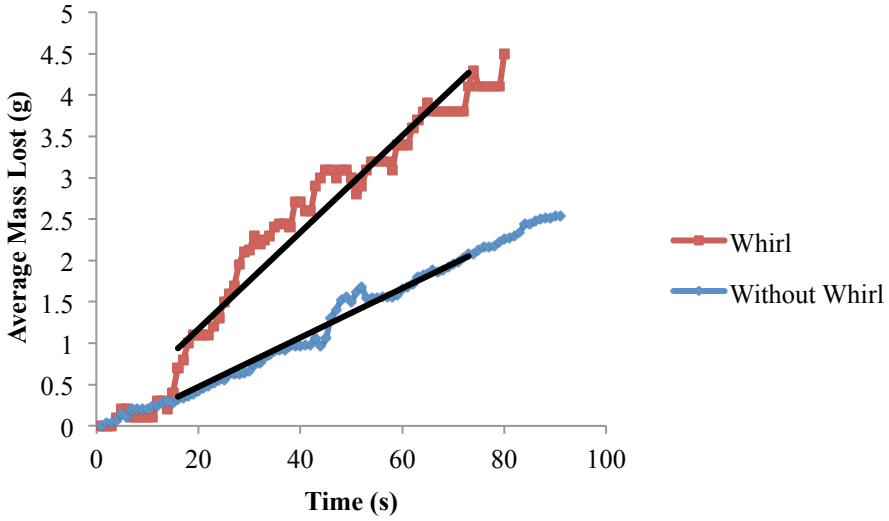

Figure 4.9. Average mass lost for 30 mL of crude oil. Lines shown represent linear fits to the middle 80% of the averaged data.

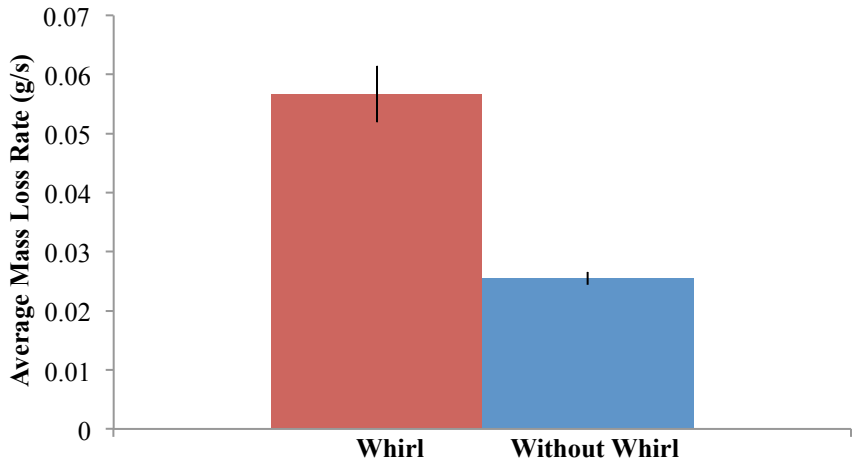

Figure 4.10. Average mass loss rate for 30 mL of crude oil.

Figure 4.11 provides a concise summary of the average mass loss rates for whirl and non-whirl experiments as a function of fuel volume. Unsurprisingly, the mass loss rate trend with the addition of a fire whirl is similar in nature to the acetone and heptane plots. Note

that the errors bars added to the "without whirl" entry are too small to discern, which is due to the small variations in mass loss rate when testing the burning rate of a simple pool fire.

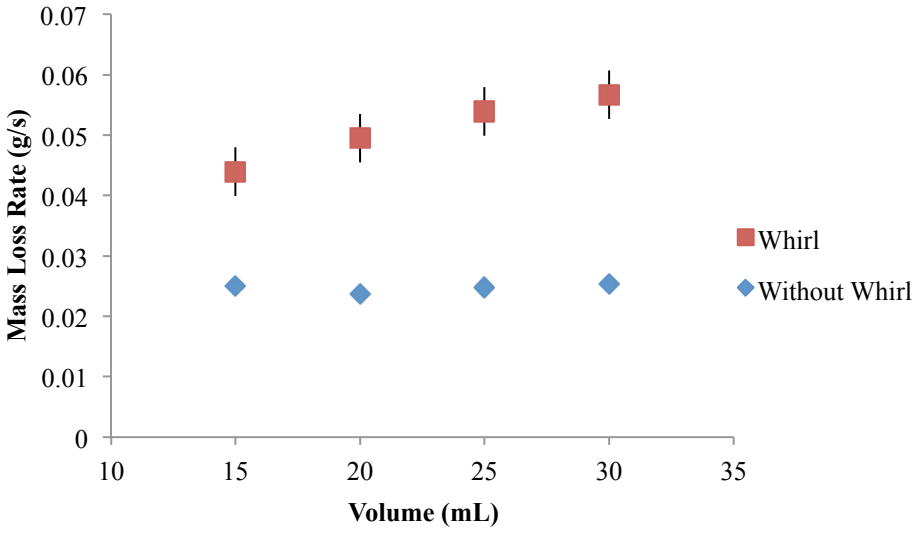

Figure 4.11. Average mass loss rate comparison for crude oil.

Figure 4.12 is a chart of the mass loss rate per unit area. To calculate this quantity, the mass loss rate that was experimentally collected was divided by the surface area of the container. As can be seen from the figure, the trend is identical to the progression illustrated in Figure 4.11, which is because the values are all divided by the same constant (12.57 cm^2). The increased volume of fuel increases the depth of the fuel layer, which affects the surface area exposed. Note that error bars are provided for both whirl and without whirl data, but they only appear for the former, as the standard deviation in mass loss rate and mass loss rate per unit area between the without whirl trials was too small.

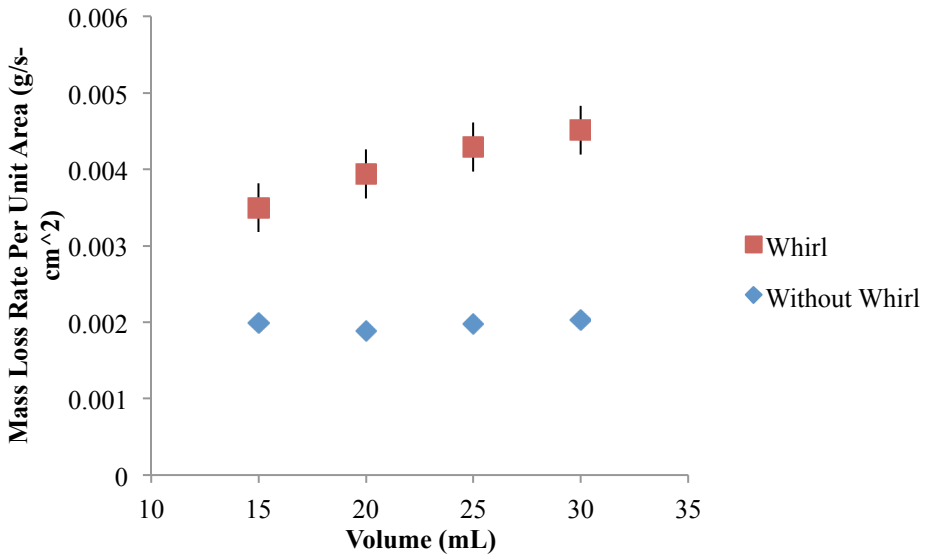

Figure 4.12. Average mass loss rate per unit area comparison for crude oil.

Figure 4.13 provides an illustration of the ratio of the mass loss rates defined in Figures 4.11 and 4.12. This plot demonstrates that the effectiveness of a fire whirl increases with increasing fuel volume because the percentage change in mass loss rate grows with crude oil volume. The increase in volume can also be interpreted as an increased in fuel depth.

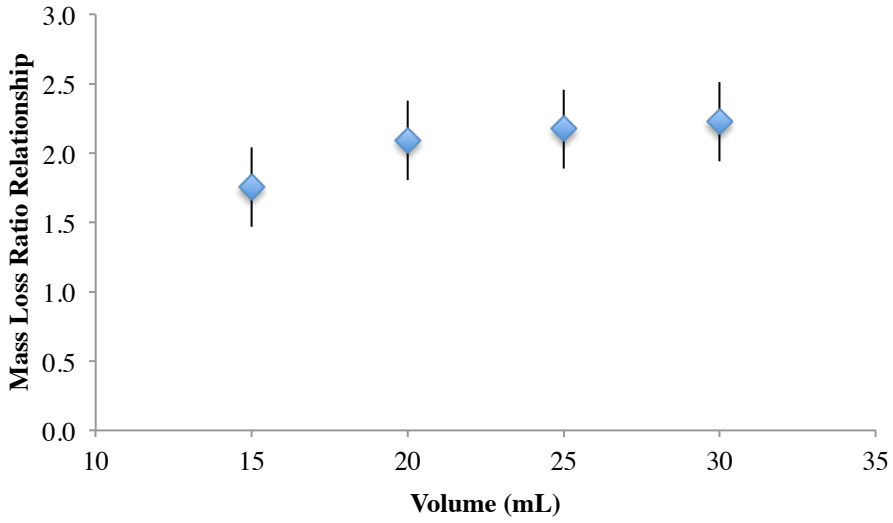

Figure 4.13. Ratio of mass loss between whirl and non-whirl for crude oil as a function of volume.

4.2 Soot Collection and Residual Fuel Results

As was mentioned previously, 3M oil absorption pads were used to collect both soot and residual fuel quantities in order to measure how a fire whirl impacts the products of combustion. Figure 4.14 is a side-by-side comparison between an absorption pad after collecting residual crude oil and a virgin pad. The first thing that stands out from this photo is the amount of crude oil that isn't consumed during the burning process. This photograph was taken after the application of a fire whirl and there still is a considerable quantity of fuel remaining. It is difficult to distinguish the outline of the pad with the black tabletop due to the sheer amount of fuel that was collected, and the small pockets of unused cloth are the only way to separate the two.

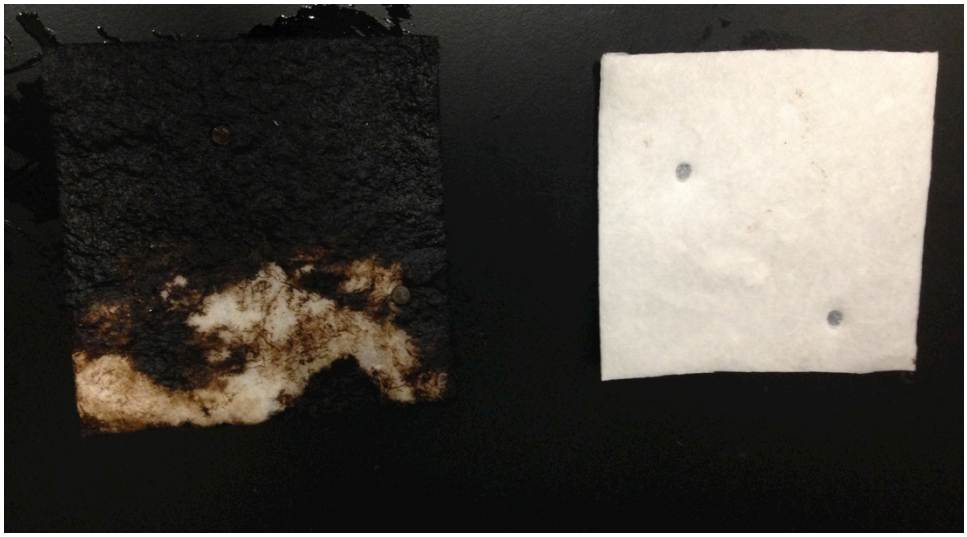

Figure 4.14. Comparison between used and unused absorption pad for residual fuel analysis.

After completing the residual fuel analysis, soot collection data was evaluated. Figure 4.15 is a picture comparing an absorption pad after collecting soot with a virgin pad.

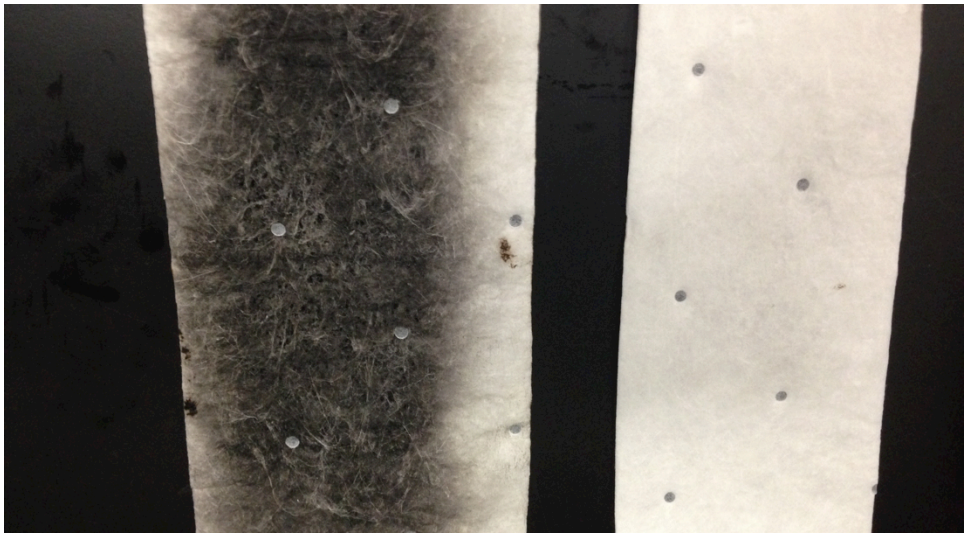

Figure 4.15. Comparison between used and unused absorption pad for soot collection analysis.

The exhaust vent is 9.5 inches long and 3.75 inches wide, so 3M absorption pads were cut accordingly to ensure that all of the soot particulates would be caught. As was the case with the residual fuel comparison, the soot collection comparison also provides a clear distinction between the before and after of a crude oil experiment. All of the soot was generated during the burning period of a 30 mL sample of oil. Using Figure 4.14 as a method of extrapolation, one can imagine the amount of soot produced during an *in situ* burn on a large oil spill. While the pictures don't provide a promising outlook as to the effectiveness of a fire whirl, the results of the subsequent soot collection and residual fuel analysis proved that fire whirls are a legitimate upgrade to the current *in situ* burning technique.

Figure 4.16 is an illustration of the percentage decrease of residual fuel with the addition of a fire whirl as a function of fuel volume. For example, when 25 mL of oil is tested, the data indicates that when a fire whirl is added, there is about 7% less residual fuel remaining than without a fire whirl. This trend steadily increases throughout the trials, which is due in part to the increased thickness of the oil layer, as it provides additional insulation from the cooler water. This provides insight into the fact that there is an ideal thickness at which testing should be completed. This thickness was not the focus of this study, and as such, necessitates additional research before a conclusive value can be provided.

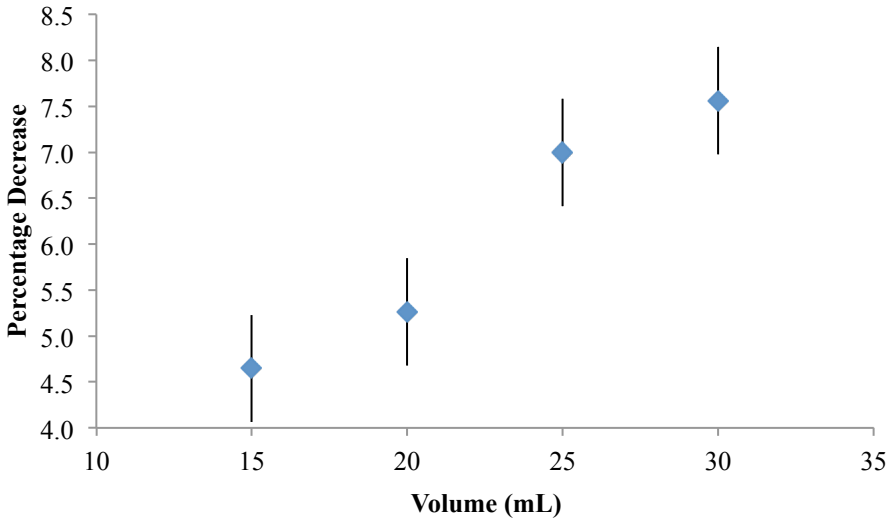

Figure 4.16. Percentage decrease of total fuel remaining as a function of fire whirl application and volume.

As can be seen from the graph, there is a definitive difference in residual fuel when a fire whirl is applied. This difference is accentuated as the volume of the fuel increases, meaning that the effectiveness of the fire whirl is amplified when more fuel is being tested. This can be attributed to an increased heat flux, supplementary radiation that stems from soot and additional fuel burning, and the subsequent increase in buoyancy, which provides greater air entrainment and a rise in the burning rate. Testing was limited to a small container with a relatively trivial amount of fuel, so it is unknown where the percentage decrease as noted as the y-axis of the figure reaches a maximum. The reason that testing could only be completed in a smaller container is due to the nature of the fire whirl and the properties of the whirling apparatus. A fire whirl produces substantial heat and energy, and as the amount of fuel is increased, so too does the heat generation. This can cause potential damage and ultimately compromise the Plexiglas fire whirl generator.

Figure 4.2 provides a close-up view of the damage that has already occurred. Because of this, the amount of fuel that could be tested had to be limited.

The data provided in Figure 4.17 correspond to the percentage decrease of soot production with the addition of a fire whirl as a function of fuel volume. For example, when 30 mL of oil are tested, the data indicates that when a fire whirl is added, there is about 17% less soot produced. The upward progression deviates between the 20 and 25 mL data points, but the overall trend indicates that increasing the fuel volume results in an increase in fire whirl effectiveness, which can be attributed to the same principles mentioned above.

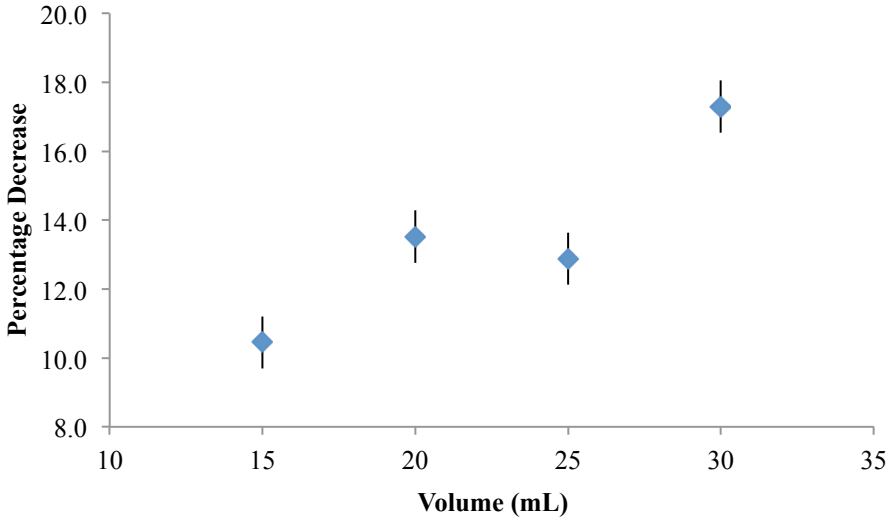

Figure 4.17. Percentage decrease of soot production as a function of fire whirl application.

The reason a larger container could not be used is due to the physical properties of the oil. For the oil to stay lit inside of the container, the entire surface of the container had to be covered with oil. If the surface was not completely covered, then pockets of water would

emerge, preventing the fire from spreading across the entirety of the surface, and subsequently cooling the surrounding oil, ultimately extinguishing the flame. For a larger container, an increased fuel volume is required to fully envelop the surface, which could potentially endanger the fire whirl generator. Combining these factors requires that the fuel volume must be limited, and in this case, to no more than 30 mL.

For an actual *in situ* burn, pockets may develop, potentially rendering any burning technique – fire whirl or not – useless. To ensure that this does not occur, the crude oil is almost always localized first. This can be done using a skimmer that collects the oil and deposits it into a location that is encircled by a boom, which prevents the oil from spreading, and ensures a fixed oil layer depth.

Tables 1-8 located in the appendix provide the data that generated Figures 4.16 and 4.17. Note that the mass before oil and soot corresponds to the mass of the absorption pad prior to experimentation, with the former representing the residual fuel and the latter the soot production. Also, the fraction of fuel remaining reflects the ratio of the amount of fuel remaining and the initial fuel. When the fire whirl is introduced, this ratio decreases meaning that more fuel is being consumed.

Chapter 5: Conclusion & Future Work

5.1 Conclusion

From the experiments performed as part of this research it was found that implementation of a fire whirl greatly increases the burning rate and total fuel consumption of fires over water. Small scale laboratory tests conducted first with acetone and heptane and later followed by experiments on crude oil show that the use of a fire whirl greatly enhances the burning rate, with increasing effectiveness as the volume of fuel is increased for the same fuel spill diameter. Exploratory experiments with heptane also showed that fires with circulation over open water burned faster than those without circulation allowed. These results all positively confirm the hypothesis that fire whirls will in fact increase the burning rate and thus effectiveness of *in situ* burning over open water, at least at laboratory scale.

Measurements of total fuel consumption vs. residual material leftover and total mass of soot released showed more efficient burning with decreased amounts of residual material and soot released during burning with a fire whirl versus a traditional pool fire configuration. If results continue to scale with a larger apparatus, fire whirls may serve as both a more efficient and environmentally friendly method of *in situ* burning. The current experiments are of course limited in their reach as the size was very small. Different controlling mechanisms may come into play at larger scales, but this preliminary work motivates future exploration of this technique at larger scales for enhanced *in situ* burning. Based on the results of this work, several potential avenues for future study are recommended below.

5.2 Future Work

One of the primary recommendations for future work would be to test in larger pool fire configurations. Some of the comparison plots of volume, ullage height, water circulation, etc. reach a plateau, meaning that the controlling variable may no longer have an affect on the results. This could be attributed to the size of the container, which, in the case of crude oil, was very limited (9-cm diameter). Increasing the size of the pan and surrounding water would help to discern the impact that it has on burning rate, efficiency, and soot production. Pool fires are known to scale with increasing size, and the fire whirls should be expected to as well. A larger container would also correspond to a bigger fire whirl generation apparatus, ultimately resulting in a larger fire whirl that would undoubtedly impact the behavior of the fire and the burning properties of the fuel. Based on the research conducted in this report, it would be appropriate to assume that increasing the size of the fire whirl would be advantageous. Increasing radiation from fires of larger sizes should increase heat fluxes to the fuel surface and therefore burning rates. Because increasing the fire size increases water circulation and air entrainment near the fuel surface, these may also contribute to an increase in the burning rate.

Another important aspect to study would be the configurations under which a fire whirl could be sustainably generated over open water. Much of the work that was reported in the literature survey involved fire whirl tests with a wind-generated configuration (L-shaped, line fire, etc.), so there is a strong possibility this can be accomplished, however the effectiveness of such a fire whirl has not yet be studied for this application. Larger, open bodies of water should also be tested to evaluate the influences of water circulation

at increasing scales. There have been reports of fire whirls forming on open bodies of water "sucking up" fuel from surrounding areas on the water, but the fuel that was burning was much less viscous, which could help the siphoning process. Whether this behavior occurs with more viscous oil should be further investigated, as it is an important factor in increasing the burning time by sustaining a large enough depth of crude oil during burning.

Evaluating fire whirls under different conditions and at a larger scale will allow for a more definitive answer to be made as to whether fire whirls are an effective alternative to the current *in situ* burning method.

Chapter 6: Appendix

Table 1. Data for 15 mL of crude oil without a fire whirl.

Mass Loss Rate (g/s)	Mass Before Oil (g)	After Oil (g)	Difference (g)	Fraction of Fuel Remaining	Mass Before Soot (g)	After Soot (g)	Difference (g)
0.028	2.43	11.77	9.34	0.79	4.97	4.98	0.013
0.027	2.99	13.69	10.7	0.89	5.37	5.38	0.012
0.024	2.6	12.02	9.42	0.78	4.96	4.97	0.011
0.024	2.48	11.49	9.01	0.77	5.06	5.08	0.015
0.023	2.86	12.6	9.74	0.83	5.26	5.28	0.016
0.025		**Average =**	**9.64**	**0.81**			**0.013**

Table 2. Data for 15 mL of crude oil with a fire whirl

Mass Loss Rate (g/s)	Mass Before Oil (g)	After Oil (g)	Difference (g)	Fraction of Fuel Remaining	Soot Before	Soot After	Difference (g)
0.048	1.8	10.88	9.08	0.73	4.36	4.37	0.015
0.034	1.89	10.67	8.78	0.74	4.55	4.56	0.01
0.045	1.95	10.91	8.96	0.75	5.42	5.44	0.012
0.045	1.81	11.35	9.54	0.80	5.16	5.17	0.012
0.049	1.76	11.37	9.61	0.85	4.52	4.53	0.011
0.044		**Average =**	**9.19**	**0.77**			**0.012**

Table 3. Data for 20 mL of crude oil without a fire whirl.

Mass Loss Rate (g/s)	Mass Before Oil (g)	After Oil (g)	Difference (g)	Fraction of Fuel Remaining	Soot Before	Soot After	Difference (g)
0.022	2.78	13.75	10.97	0.69	5.29	5.31	0.019
0.024	2.71	11.56	8.85	0.55	5.36	5.37	0.019
0.024	2.73	11.75	9.02	0.58	5.34	5.36	0.024
0.024	2.23	10.74	8.51	0.54	5.19	5.22	0.024
0.024	2.35	12.34	9.99	0.64	5.03	5.05	0.025
0.024		**Average =**	**9.47**	**0.60**			**0.022**

Table 4. Data for 20 mL of crude oil with a fire whirl.

Mass Loss Rate (g/s)	Mass Before Oil (g)	After Oil (g)	Difference (g)	Fraction of Fuel Remaining	Soot Before	Soot After	Difference (g)
0.051	1.86	11.35	9.49	0.60	4.51	4.53	0.012
0.048	2.5	11.69	9.19	0.56	5.34	5.36	0.022
0.058	1.76	10.19	8.43	0.55	5.18	5.20	0.019
0.043	1.79	10.95	9.16	0.57	4.65	4.67	0.022
0.046	2.71	11.28	8.57	0.55	5.18	5.20	0.021
0.050		**Average =**	**8.97**	**0.57**			**0.019**

Table 5. Data for 25 mL of crude oil without a fire whirl.

Mass Loss Rate (g/s)	Mass Before Oil (g)	After Oil (g)	Difference (g)	Fraction of Fuel Remaining	Soot Before	Soot After	Difference (g)
0.024	2.4	14.48	12.08	0.60	5.59	5.61	0.027
0.025	2.83	15.49	12.66	0.63	7.38	7.41	0.033
0.025	2.49	16.17	13.68	0.71	5.80	5.82	0.024
0.025	2.51	14.04	11.53	0.60	5.81	5.83	0.022
0.026	2.14	14.6	12.46	0.61	6.35	6.37	0.026
0.025		**Average =**	**12.48**	**0.63**			**0.026**

Table 6. Data for 25 mL of crude oil with a fire whirl.

Mass Loss Rate (g/s)	Mass Before Oil (g)	After Oil (g)	Difference (g)	Fraction of Fuel Remaining	Soot Before	Soot After	Difference (g)
0.054	2.28	14.47	12.19	0.63	8.57	8.59	0.021
0.057	2.7	14.33	11.63	0.57	9.86	9.88	0.024
0.054	1.85	13.1	11.25	0.56	9.76	9.78	0.023
0.053	2.36	14.42	12.06	0.60	9.16	9.18	0.023
0.051	2.24	13.44	11.2	0.56	9.56	9.58	0.024
0.054		**Average =**	**11.67**	**0.59**			**0.023**

Table 7. Data for 30 mL of crude oil without a fire whirl.

Mass Loss Rate (g/s)	Mass Before Oil (g)	After Oil (g)	Difference (g)	Fraction of Fuel Remaining	Soot Before	Soot After	Difference (g)
0.024	2.84	18.76	15.92	0.65	5.74	5.78	0.035
0.025	2.46	17.86	15.4	0.64	4.51	4.54	0.034
0.026	2.26	18.12	15.86	0.66	5.44	5.48	0.041
0.026	2.72	17.88	15.16	0.64	5.91	5.95	0.038
0.027	3.23	18.92	15.69	0.64	6.71	6.75	0.037
0.025		**Average =**	**15.61**	**0.65**			**0.037**

Table 8. Data for 30 mL of crude oil with a fire whirl.

Mass Loss Rate (g/s)	Mass Before Oil (g)	After Oil (g)	Difference (g)	Fraction of Fuel Remaining	Soot Before	Soot After	Difference (g)
0.065	2.02	16.45	14.43	0.63	9.05	9.08	0.03
0.054	3.84	18.44	14.6	0.59	8.82	8.85	0.032
0.054	2.4	16.8	14.4	0.60	8.29	8.32	0.031
0.056	3.04	17.55	14.51	0.60	9.54	9.57	0.029
0.055	2.1	16.07	13.97	0.58	7.60	7.63	0.031
0.057		**Average =**	**14.38**	**0.60**			**0.031**

References

[1] Jarvis, Alice-Azania. "BP Oil Spill: Disaster by Numbers." *The Independent*. Independent Digital News and Media, 14 Sept. 2010. Web. 09 Sept. 2014.

[2] Repanich, Jeremy. "The Deepwater Horizon Spill by the Numbers" *Popular Mechanics*. N.p., 10 Aug. 2010. Web. 10 Sept. 2014.

[3] Clark, Josh. "How Do You Clean Up an Oil Spill?" *HowStuffWorks*. HowStuffWorks.com, n.d. Web. 06 Oct. 2014.

[4] Maksim, J., Jr. "Patent US3702297 - Oil Skimming Device and Method." *Google Books*. N.p., 1972. Web. 04 Oct. 2014.

[5] The Editors of Encyclopædia Britannica. "Oil Spill." *Encyclopedia Britannica Online*. Encyclopedia Britannica, n.d. Web. 04 Oct. 2014.

[6] "Dispersing Agents." *Dispersing Agents*. EPA, 27 May 2014. Web. 05 Oct. 2014.

[7] Ayre, James. "New Ecologically Friendly Way To Clean Up Oil Spills — Raw Unprocessed Cotton." *CleanTechnica*. N.p., 21 May 2013. Web. 10 Sept. 2014.

[8] Liggett, Brit. "Naturally Occuring Bacteria Could Help Clean Oil Spill."*Inhabitat Sustainable Design Innovation Eco Architecture Green Building Naturally Occuring Bacteria Could Help Clean Oil Spill Comments*. N.p., 3 May 2010. Web. 10 Sept. 2014.

[9] Griggs, Mary Beth. "How Microbes Help Clean Our Environment." *Popular Mechanics*. N.p., 29 Aug. 2011. Web. 10 Sept. 2014.

[10] Waldie, Paul. "A Canadian Solution to the Gulf Oil Spill." *The Globe and Mail*. N.p., 23 Aug. 2010. Web. 10 Sept. 2014.

[11] Michel J., D. Scholz, S. R. Warren, and A. H. Walker. *A Decision-Makers Guide to* In-*Situ Burning.* Rep. No. 4740. American Petroleum Institute, April 2005.

[12] Buist, Ian, James Mccourt, Steve Potter, Sy Ross, and Ken Trudel. "In Situ Burning." *Pure and Applied Chemistry* 71.1 (1999): 43-65. Web.

[13] Brogaard, N.L., Sørensen, M.X., Fritt-Rasmussen, J., Rangwala, A.S., and Jomaas, G. *A New Experimental Rig for Oil Burning on Water - Results for Crude and Pure Oils*. in Proc. Fire Safety Sci. 2014. Canterbury, New Zealand, Feb 10-14, 2014.

[14] Buist, Ian. "Window-of-Opportunity for In Situ Burning." *Spill Science & Technology Bulletin* 8.4 (2003): 341-46. Web.

[15] "Join Industry Oil Spill Preparedness and Response Task Force." (2010): 1-2. *Http://www.chevron.com/documents/pdf/SpillPreparednessResponseRecommendations.pdf*. JTIF, API, IADC, IPAA, NOIA, and USOGA, 3 Sept. 2010. Web.

[16] Garo, J.p., J.p. Vantelon, S. Gandhi, and J.l. Torero. "Determination of the Thermal Efficiency of Pre-boilover Burning of a Slick of Oil on Water." *Spill Science & Technology Bulletin* 5.2 (1999): 141-51. Web.

[17] Wu, Neil, Michael Baker, Gilles Kolb, and Jose L. Torero. "Ignition, Flame Spread and Mass Burning Characteristics of Liquid Fuels on a Water Bed." *Spill Science & Technology Bulletin* 3.4 (1996): 209-12. Web.

[18] Walavalkar, A.y, and A.k Kulkarni. "Combustion of Water-in-oil Emulsion Layers Supported on Water." *Combustion and Flame* 125.1-2 (2001): 1001-011. Web.

[19] "Guidelines for Inshore/Nearshore In-Situ Burn." 1-2. NOAA. Web. 10 Sept. 2014.

[20] "Oil Spills Fast Facts." *CNN*. Cable News Network, 08 Sept. 2014. Web. 10 Sept. 2014.

[21] "Questions About Environmental Tradeoffs." *Questions About Environmental Tradeoffs*. NOAA, 29 Dec. 2000. Web. 10 Sept. 2014.

[22] "B.C. Air Quality." *The Impacts of Ozone Depletion*. Environment Canada, n.d. Web. 10 Sept. 2014.

[23] Shinohara, Masahiko, and Sanae Matsushima. "Formation of Fire Whirls: Experimental Verification That a Counter-rotating Vortex Pair Is a Possible Origin of Fire Whirls." *Fire Safety Journal* 54 (2012): 144-53. Web.

[24] Countryman, Clive M. "Fire Whirls... Why, When, and Where." (1971): 3-14. *Pacific Southwest Forest and Range Experimental Station*. Web.

[25] Kuwana, Kazunori, Kozo Sekimoto, Kozo Saito, Forman A. Williams, Yoshihiko Hayashi, and Hideaki Masuda. "Can We Predict the Occurrence of Extreme Fire Whirls?" *AIAA Journal* 45.1 (2007): 16-19. Web.

[26] Kuwana, Kazunori, Kozo Sekimoto, Kozo Saito, and Forman A. Williams. "Scaling Fire Whirls." *Fire Safety Journal* 43.4 (2008): 252-57. Web.

[27] Graham H. E., “Fire-whirlwind formation as favored by topography and upper winds,” *Fire Control Note*, vol. 18, pp. 20-24, 1957.

[28] Emmons, Howard W., and Shuh-Jing Ying. "The Fire Whirl." *Symposium (International) on Combustion* 11.1 (1967): 475-88. Web.

[29] Zhou, Rui, and Zi-Niu Wu. "Fire Whirls Due to Surrounding Flame Sources and the Influence of the Rotation Speed on the Flame Height." *Journal of Fluid Mechanics* 583 (2007): 313. Web.

[30] Battaglia, F., McGrattan, L. B., Rhem, R. G. & Baum, H. R. 2000a Simulating Fire Whirls. *Combust. Theory Model.* 4, 123-138.

[31] Satoh, K. & Yang, K. T. 1996 Experimental Observations of Swirling Fire. In *Proc. 1996 ASME Intl. Mechanical Engineering Congress and Exposition. Part 1,* 393-400. ASME.

[32] Farouk, B., Department Of Mechanical Engineering And Mechanics, Drexel University, and Pa Philadelphia. "Large Eddy Simulation of Naturally Induced Fire Whirls in a Vertical Square Channel with Corner Gaps." 3-9. NIST, Nov. 2000. Web.

[33] Vyalykh, D. V., A. E. Dubinov, D. Yu. Kolotkov, I. L. L'Vov, S. A. Sadovoi, and E. A. Sadchikov. "A Portable Hand-driven Solid-fuel Device for Generating Fire Whirls." *Instruments and Experimental Techniques*56.3 (2013): 347-48. Web.

[34] Grishin, A.M., Reino, V.V., Sazanovich, V.M., Tsvyk, R.Sh., and Sherstobitov, M.V., *Russ. Phys. J.*, 2012, vol. 54, p. 1311.

[35] Kuwana, Kazunori, Kozo Sekimoto, Takeaki Minami, Takahiro Tashiro, and Kozo Saito. "Scale-model Experiments of Moving Fire Whirl over a Line Fire." *Proceedings of the Combustion Institute* 34.2 (2013): 2625-631. Web.

[36] Emori, R. I. & K. Saito, *Fire Technology*. 18 (1982): 319-27.

[37] "The Naked Scientists." *Science Podcasts*. N.p., 14 Mar. 2010. Web. 10 Sept. 2014.

[38] Arai, M., Saito, K., Altenkirch, R.A., 1990. A study of boilover in liquid pool fires supported on water Part I: effect of a water sublayer on pool fires. Combustion Science and Technology 71, 25–40.

[39] Ito, A., Saito, K., Inamura, T., 1992. Holographic interferometry temperature measurements in liquids for pool fires supported on water. Transactions of the ASME 114, 944.

[40] Garo, J.P., Vantelon, J.P., Fernandez-Pello, A.C., 1996. Effect of the fuel boiling point on the boilover burning of liquid fuel spilled on water. In: Twenty-sixth Symposium (International) on Combustion, The Combustion Institute, pp. 1461–1467.

[41] Koseki, H., Kokkala, M., Mulholland, G.W., 1991. Experimental study of boilover in crude oil fires. In: Fire Safety Science- Proceedings of the Third International Symposium, pp. 865–875.